CRUSTAL MODELLING FROM GRAVITY DATA IN THE ETHIOPIAN RIFT

by

ABERA ALEMU

A Thesis

Submitted to the

School of Graduate Studies

and

the Faculty of Science in the

Addis Ababa University

In Partial Fulfillment

of the Requirements for the Degree

Master of Science in Physics

June 1983

ACKNOWLEDGEMENTS

My thanks are due in the first place to Ato Getahun Demisse, Director of the Ethiopian Geological Survey, Ministry of Mines and Energy, Addis Abeba on whose suggestion I took up this project as part of my thesis. The coming of this paper to its final stage is the result of the initiative and unfailing support of the Ministry in general and the director in particular. I was given access to use all the materials I needed including transport both to carryout the field work and to bring this paper to its final stage.

I am greatful to my advisor Dr. Laike Mariam Asfaw (Director of the Geophysical Observatory) for giving his valuable time to go through the first draft and criticizing it constructively and guiding throughout the progress of the paper.

I greatfully acknowledge all those members of the Langano Geothermal Prospect who contributed to this work particularly, Ato Abiye Hunegnaw field manager of the Geothermal - Geophysics Division, Ato Solmon Abera Surveyor and all members of the geophysical team for being very cooperative when their help was needed.

My acknowledgement also goes to Prof. M.P. Hochestein Geothermal Institute, University of Auckland, N.Z., Ato Getahun Demisse, Ato Befekadu Oluma and Mr. T. Kenan UNDP expert in the Ministry of Mines and Energy, Ethiopia for many useful discussions, suggestions and interpretations.

I greatly acknowledge the help given to me by the Cartographic Section of the Geological Survey, particularly Ato Negussie Teshome and Ato Awetahagn in drafting the figures, Ato Alemu and Ato Lisanu in reducing and producing blue print copies of the figures. My thanks are due to my sister w/t Zerfinesh Mekasha who helped in reducing the data and organizing the notes, w/t Almaz Armide who typed the manuscript carefully and legibly and Ato Asefa computer-technician for his kind help in running the computer during generation of the models.

C O N T E N T S

ILLUSTRATIONS

Page

List of figures

List of tables

ABSTRACT

A detailed gravity survey of the Main Ethiopian Rift Valley between latitudes $7^{\circ}N$ and $8^{\circ}N$, has shown that there is a broad relative positive Bouguer anomaly over the whole of the Rift floor, and this anomaly is superimposed on the regional, broad negative anomaly of the Ethiopian and Somali Plateau. The broad relative positive anomaly over the rift floor is between 60 and 100 km wide and has an amplitude of 30 - 60 mgal. On the broad relative positive anomaly over the rift floor are superimposed other short-wave length relative positive anomalies which seem to be situated along the displacement lines of the Wonji Fault Belt. There are also much narrower relative positive anomalies along the margins of the rift other than those associated with the Wonji Fault Belt.

In their interpretation of the gravity minimum near the center of profile C (page 47), Searle and Gouin (1972) suggested that this gravity minimum is due to low density lavas of the Aluto volcano and they further associated the volcano with a small negative anomaly. On the contrary the present survey shows that the volcano is associated with a relative positive anomaly of magnitude comparable to the short-wave length relative positive anomalies along the displacement lines of the Wonji Fault Belt.

Due to both, denser spacings of gravity stations and quality of data, it is believed that the present gravity survey of the Main Ethiopian Rift between latitudes $7^{\circ}N$ and $8^{\circ}N$ defines more

accurately the location of the gravity anomalies (both the negative and the positive anomalies). The priliminary interpretations of the gravity anomalies made in this work are corroborated by bore hole data (Figs. 10, 11) and surface geology (Fig. 2) of the study area. Furthermore, inferred density measurements on surface rocks and Cores from production bores in the Olkaria geothermal field of Kenya (Table 2) have been utilized.

1. Introduction

The Central Part of the Main Ethiopian Rift Valley (Fig. 1) is an important part of the Main Ethiopian Rift which forms the East African Rift System which has long been recognized as part of the World Rift System.

Prior to the gravity survey carried out in this work, reconnaissance gravity surveys carried out in Ethiopia (Gouin and Mohr, 1964; Gouin 1970) and detailed gravity survey carried out in the Central Part of the Main Ethiopian Rift (Searle and Gouin, 1972) have shown that:

1. The Ethiopian and Somali plateau are associated with broad negative Bouguer anomalies.
2. Within the Main Ethiopian Rift, on the broad negative regional anomaly, is superimposed a relative broad positive anomaly. On this broad positive anomaly, which covers most of the rift, much narrower relative positive Bouguer anomalies are superimposed locally.

The broad negative anomaly is thought to be caused by low density upper mantle (possibly astenosphere) underlying the Ethiopian high lands (Searle and Gouin, 1971, 1972). On the other hand the broad positive anomaly and the locally superimposed much narrower positive anomalies within the Main Ethiopian Rift were interpreted as being caused by high density intrusions (Searle and Gouin, 1972) and intrusions

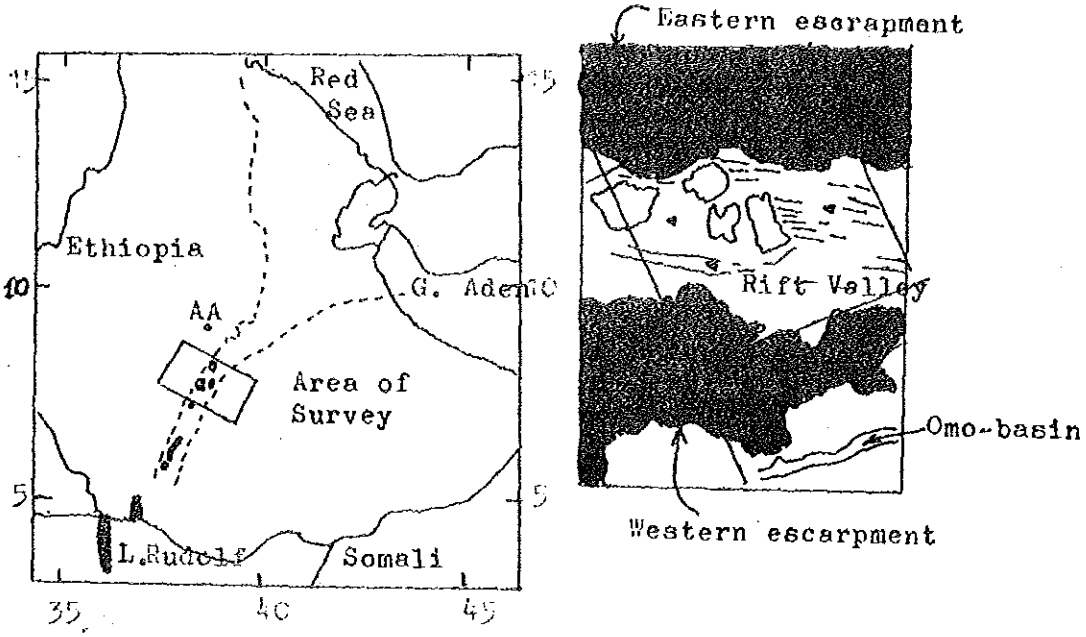

Fig. 1. Location of Survey area.

associated with the Wonji Fault Belt (Gouin and Mohr, 1964) respectively.

The present work describes the results of 400 new gravimeter observations and some of the previous observations of Searle and Gouin (1972) in the Central Part of the Main Ethiopian Rift. The results are presented in the form of tables of principal facts and preliminary gravity anomaly maps.

The gravity stations with their coordinates and elevation values have been classed as A, B and C (Appendix I) depending

upon their accuracy.

The geological interpretation is based upon the Bouguer anomalies, Borehole data and known surface geology. Density contrasts used in the interpretation were infered from density measurements made on surface rock samples and cores from production wells of the Olkaria Geothermal field in Kenya.

This survey was undertaken with following aims:

1. To present reliable data which will form a sound basis for further investigation of the rift.
2. To produce preliminary Bouguer, residual and regional anomaly maps of the region and locate the gravity anomalies associated with the rift as accurately as possible.
3. To compare the results of this survey with those carried out by Searle and Gouin. Especially this is important in view of the fact that Searle and Gouin (1972) consider their work to be of preliminary nature.
4. To generate simple models that produce the gravity anomalies matching the geological and geophysical data.

2.0 Geology of the Central Part of the Main Ethiopian Rift Valley (Lakes District).

Since the initial work of Mohr (1960), geological knowledge of the Central Part of the Main Ethiopian Rift Valley (CPMERV) between latitudes 7°N and 8°N or the Lakes District (LD) has been enlarged as a result of prospecting work by the Ethiopian Institute of Geological Survey (EIGS) in the "Detailed Investigation Phase of Geothermal Resources for Power Development". The result is that the geology in the CPMERV is fairly known.

2.1 Geological Setting

Along its 400 km length, the Main Ethiopian Rift Valley has a gently curvillinear plan, convex to the west (Fig. 1). To become identified with South western Afar, the rift valley widens out at its northern end. At the southern end, crustal extensions are transposed west into the seismically and tectonically active region of the middle Omo-basin.

The Main Ethiopian Rift Valley maintains a width of 80 ± 15 km along most of its length and 65 ± 10 km in the central part. A major watershed at 1680 m elevation crosses the rift floor at latitude 9°N and separates the Awash Valley and Afar to the north from the Central Part of the Main Ethiopian Rift Valley to the south. The CPMERV contains four large lakes (Ziway, Langano, Shalla and Abiyata) (Fig. 2).

The floor of the CPMERV declines gradually Southwards until a terminal sink is reached at the 1560 m elevation of Lake Shalla. The rest of the Main Ethiopian Rift Valley, South and West of the Central Part, is occupied by the Billati-Sagan drainage system (Fig. 2). The Billati river flows due south from sources on the western escarpment overlooking the CPMERV.

2.2 Structure

The Main Ethiopian Rift Valley commenced to form during late tertiary period (Lloyd, 1977). The rift is essentially a graben formed by drifting of the Ethiopian plate to the west and the Somali plate to the east through tensional normal faulting .

During tertiary time there was a series of regional up lifts and by the pleistocene (Baker et al. 1976) the protorift was a topographically shallow trough with deep infilling of silicic volcanics erupted from centers close to the rift margins. Mohr (1966 b) suggests that the marginal faults are pleistocene in age and that the separation of the Ethiopian plate to the west and the Somali plate to the east occured at this time.

By late pleistocene - Holocene subsequent tectonic fragmentation of the rift floor formed the youngest structural deformation, largely concentrated within a narrow, 8 ± 2 km wide belt of normal faulting, known as the Wonji Fault Belt (WFB) (Mohr, et al., 1980; Lloyd 1977).

The WFB maintains a NNE orientation along the entire length of the Main Ethiopian Rift Valley and has been forced into en-echelon offsets inorder to remain within the rift margin envelope. In the Central Part of the Main Ethiopian Rift, the WFB runs close or adjacent to the eastern margin and tends to be axial between the rift margins along the whole length of the Main Ethiopian Rift.

Within the CPMERV or Lakes District between latitudes $7^{o}N$ and $8^{o}N$, the WFB is divided into three segments, named from south to north, Corbetti-Shalla, Shalla - Ziway and East Ziway, by two en-echelon offsets (Lloyd, 1977). The Corbetti -Shalla and East Ziway segments coincide with basaltic volcanic provinces where Volcanism is not extinct.

2.3 Volcanism and Rocks Flooring the Area.

A notable feature of the Main Ethiopian Rift is the occurence of young volcanic centers along all except its most southern part. Volcanism in the CPMERV is of pleistocene and holocene age (Mohr 1960, 1966a, 1966b, Lloyd 1977). Rhyolite volcanism on the rift floor of the CPMERV is concentrated in four centers (Fig. 2), Gademota Caldera, Aluto Volcanic Center, Shalla Volcanic Center and Corbetti Volcanic Center. The rift floor is partially infilled with lacustrine sediments derived from quaternary volcanic rocks of pleistocene and holocene age. Contemporaneous with the volcanism the infill consists of intercalations of siltstone, claystone, pumices, etc.

Ephemeral lakes have also occupied the CPMERV since the earliest stages of its development and these lakes contributed sediment to the floor. Volcanic rocks, erupted from centers within and outside the rift are interbeded with the sediments.

The sediments are underlain by rhyolites, ignimbrites trachytes, agglomerates and basalts of the upper miocene to pleistocene age and outcrop at the eastern and western edges of the lake sediments and cover wide areas upto the tops of the rift scraps. The tops of the rift scarps are covered extensively by trap basalts of the peleocene to lower miocene age. These trap basalts are supposed to underlie rhyolites, trachytes, ignimbrites, agglomerates and basalts of the upper miocene to pleistocene age in the rift floor.

Fissure basalts and scoria cones are common at the East Ziway and Corbetti - Shalla segments but are absent from the Shalla - Ziway segment of the WFB (Lloyd, 1977).

3.0 Theoretical basis of gravity methods.

Newton's law of universal gravitation may be stated as follows: The mutual gravitational attraction between two particles having masses m_1 and m_2 which are separated by a distance r has the value

$$F(r) = Gm_1m_2/r^2 \qquad (3.1)$$

and acts in the direction of r. The force per unit mass on a particle at any point P at a distance r from m_1 is defined as the gravitational field of the particle m_1. This is written as:

$$\vec{F} = -G\, m_1\vec{r}/r^3 \qquad (3.2)$$

Such a field is conservative, and is therefore derivable from a scalar potential function V(r) as follows

$$\vec{F}(r) = -\vec{W}(r) \qquad (3.3)$$

where $V(r) = -Gm_1/r$ is the gravitational potential of the mass m_1.

The gravitational potential, due to a continuous distribution of matter with density ρ and volume v at any exterior point P is

$$V_p(r) = -\int_v \frac{Gdm}{r} \qquad (3.4)$$

where $dm = \rho\, dv$

If the volume integration is carried out over the entire earth, one obtains the earth's gravitational potential in free

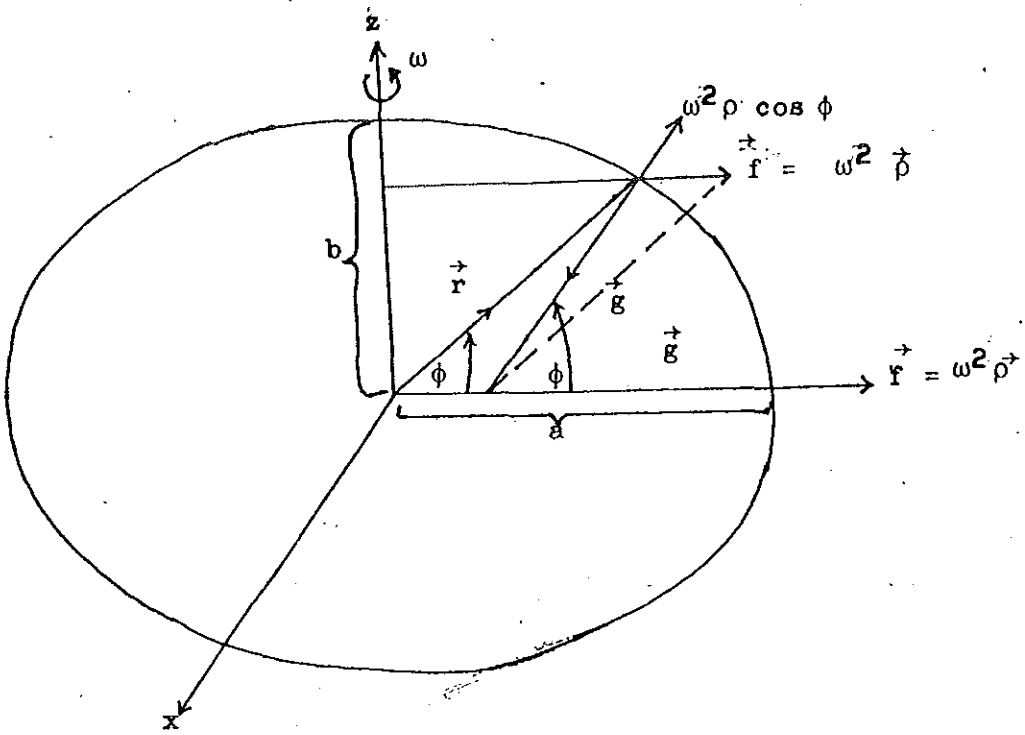

Fig. 3a Vector of centrifugal force, gravitational force and resultant force.

space, from which the gravitational field may be found by differentiation. If P is on the earth's surface, the gravitational field there is denoted by the symbol g.

The force acting on a particle at rest on the earth's surface is the resultant of the gravitational force and the centrifugal force of the earth's rotation. The centrifugal force on a unit mass is given by

$$\vec{f} = \omega^2 \vec{\rho} \qquad (3.5)$$

where ω is the angular velocity of rotation and ρ is the distance from the axis of rotation to the point mass.

In vector form it can be shown that

$$\vec{f} = (\omega^2 x, \omega^2 y, o) \tag{3.6}$$

and this force can be derived from a potential

$$\Psi = \tfrac{1}{2}\omega^2 (x^2 + y^2) \tag{3.7}$$

so that

$$\vec{f} = \vec{\nabla}\Psi \tag{3.8}$$

The total force, the resultant of the gravitational force and centrifugal force is called gravity. The potential of gravity (Geopotential), U, is the sum of the potentials of gravitational force and the centrifugal force, i.e.

$$U = V + \Psi \tag{3.9}$$

which can be expressed as

$$U = G \int_V dm/r + \tfrac{1}{2}\omega^2 (x^2 + y^2) \tag{3.10}$$

The gravity vector is related to U by

$$\vec{g} = (g_x, g_y, g_z) = -\vec{\nabla}U \tag{3.11}$$

The surfaces

$$U = \text{constant} = C \tag{3.12}$$

On which the potential U is a constant are called equipotential surfaces.

If the vector $\vec{ds}$ = (dx, dy, dz) is taken

along an equipotential surface the work done is

$$dU = \vec{\nabla} U . \vec{ds} = 0 \qquad (3.13)$$

so that $\vec{\nabla}U$ and $\vec{ds}$ are perpendicular to one another i.e the gravity vector, $\vec{g}$, is normal to the surface. Introducing spherical polar coordinates (r, ϕ) in the second term of equation (3.10) and noting that $(x^2 + y^2) = \rho^2 = r^2\cos^2\phi$ (Fig. 3a) we have

$$U(r,\phi) = G \int \frac{dm}{r} + \tfrac{1}{2}\omega^2 r^2 \cos^2\phi \qquad (3.14)$$

where ϕ is the geocentric latitude.

Since C is arbitrary, with an appropraite choice of parameters $r = a$, equatorial radius of the earth and $\phi = 0$ equatorial latitude, equation (3.14) will have the form

$$U(a,0) = G \left[\int_V \frac{dm}{r} \right]_{r=a} + \tfrac{1}{2}\omega^2 a^2 = C \qquad (3.15)$$

Equating this value of C to equation (3.10) we get

$$G \int_V \frac{dm}{r} + \tfrac{1}{2}\omega^2 \rho^2 = G \left[\int_V \frac{dm}{r} \right]_{r=a} + \tfrac{1}{2}\omega^2 a^2 \qquad (3.16)$$

which is the equation of an equipotential surface very close to that of earth at sea level. This surface is known as the geoid.

To obtain expressions valid to the desired order of small quantities, it is usual to expand the integral on the left hand side of equation (3.16) into a series in (r, ϕ).

This may be done by expanding the cosine law expression for 1/r (fig. 3b) as follows.

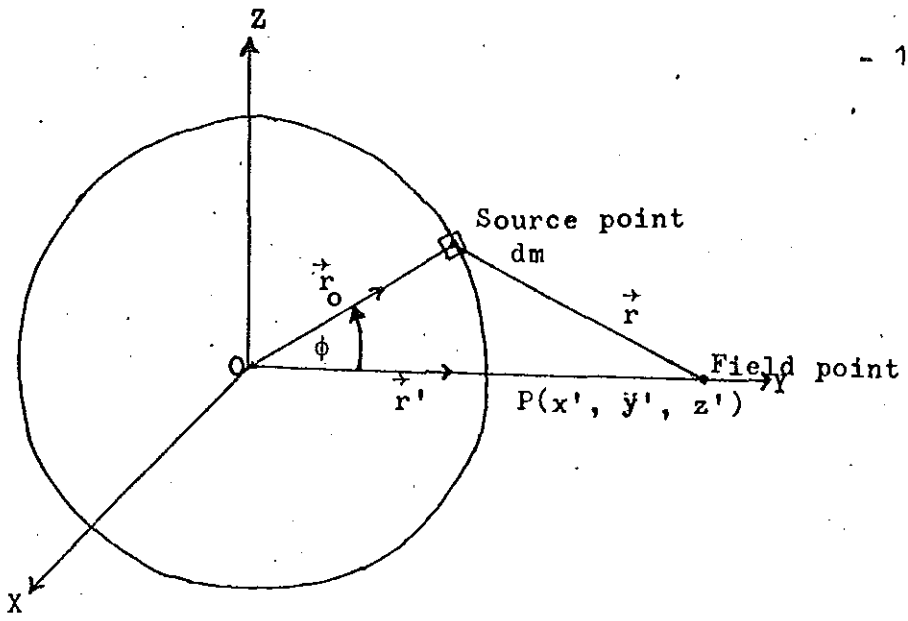

Fig. 3b Notation for the development of gravity on a spheroid .

$$1/r = 1/r' \sum_{n=0}^{\infty} (r_o/r')^n \; P_n(\cos \phi) \qquad (3.17)$$

where $P_n(\cos\phi)$ is the Legendre polynomial. Substituting this value of 1/r into the left hand side of equation (3.16) we get

$$U(r,\phi) = G \int_v dm \left[1/r' \sum_{n=0}^{\infty} (r_o/r')^n \; P_n(\cos\phi) \right] + \tfrac{1}{2}\omega^2(x'^2+y'^2) \qquad (3.18)$$

If we retain only the first three terms in equation (3.18) above we have

$$U(r, \phi) = G/r' \left[\int_v dm + 1/r' \int_v P_1(\cos\phi) r_o dm + 1/r'^2 \int_v P_2(\cos\phi) r_o^2 dm \ldots \right] + \tfrac{1}{2}\omega^2(x'^2 + y'^2) \qquad (3.20)$$

In the expression for U of equation (3.20) above the first

integral gives M, the mass of the earth, the second will evidently reduce to a series of first moments about O, and therefore vanish (since O is the center of mass), and the thrid will reduce to a sum of moments and products of inertia. If we select x and y - axes to be the principal axes of inertia, so that products of inertia vanish, and let A, B and C be moments of inertia about x, y and z respectively.

Then

$$\int P_2(\cos\phi)\, r_o^2 dm = 3/2\ (C - \frac{A+B}{2})\ (1-\sin^2\phi) \qquad (3.21)$$

and the expression for U may be written as

$$U(r,\ \phi) = MG/r\ \ 1+\frac{K}{2r^2}(1-3\sin^2\phi) + \frac{\omega^2 r^2}{2MG}\cos^2\phi \qquad (3.22)$$

where $K = (C - \frac{A+B}{2})/M$

We know introduce the condition that the external surface (Fig. 3b) is an equipotential surface, $U(r,\phi) = U_o$, and that P lies on it. Then the shape of the surface is defined by

$$r = MG/U_o\ \left[1 + \frac{K}{2a^2}\ (1-3\sin^2\phi)\right] + \frac{\omega^2 a^2}{2MG}\cos^2\phi \qquad (3.23)$$

where the equatorial radius a has been substituted for r in the second and third terms.

The term $\frac{\omega^2 a^3}{MG}$ may be denoted by m, where

$$m = a\omega^2 / (MG/a^2) \qquad (3.24)$$

Equation (3.24) indicates the ratio of the centripetal

acceleration at equator to attraction at equator. Substituting m into equation (3.23) and rearranging, we have

$$r = MG/U_o\left(1 + \frac{K}{2a^2} + \frac{m}{2}\right)\left[1-\left(\frac{3K}{2a^2} + \frac{m}{2}\right)\right]\sin^2\phi \qquad (3.25)$$

which is of the form

$$r = a(1 - q\sin^2\phi) \qquad (3.26)$$

and is an equation for the surface of a spheroid.

The quantity q is given by

$$\frac{\text{equatorial radius - polar radius}}{\text{equatorial radius}}$$

and is known as the flattening of the spheroid.

Therefore,

$$q = \frac{3K}{2a^2} + \frac{m}{2} \qquad (3.27)$$

Gravity at any distance r is given to the first order by

$$\vec{g} = -\partial U/\partial r \ \hat{e}_r$$

or

$$g = MG/r^2 \left[1 + 3K/2r^2 (1-3\sin^2\phi) - m\cos^2\phi\right] \qquad (3.28)$$

and gravity on the spheroid, γ_o, is obtained by substituting the value of r from equation (3.26) i.e

$$\gamma_o = -\partial U/\partial r \Big|_{r = a(1-q\sin^2\phi)}$$

or

$$\gamma_o = U_o^2/MG\left(1 + \frac{K}{2a^2} - 2m\right)\left[1+\left(2m - \frac{3K}{2a^2}\right)\right]\sin^2\phi \qquad (3.29)$$

This is of the form

$$\gamma_o = \sum_{n=0}^{\infty} a_n \sin^2 n\phi \qquad (3.30)$$

where the conefficients a_n are chosen by fitting world-wide, pendulm measurements of gravity, which have been reduced to sea level. It turns out (on the basis of data existing in 1930) that $a_o = 978.0490$ gals; $a_1 = 0.0052884\ a_0$; $a_2 = -0.0000059\ a_o$ and a_3 and succeeding coefficients are insignificant. Thus the variation of the main gravitational field (theoretical gravity) with latitude on the reference spheroid is described by the formula

$$\gamma(\phi) = 978.0490\ (1+0.0052884\ \sin^2\phi - 0.0000059\ \sin^2 2\phi)\ \text{gals} \quad \ldots \quad (3.31)$$

This formula may be used to correct all gravity data for the ellipticity of the earth.

Since the earth has not been able, in the course of its evolution, to preserve homogeneity even on its concentric spheroid, disturbances in the g-field occur. This disturbances are called anomalies defined by

$$\Delta g = g_o - \gamma_o \quad - \quad (3.32)$$

where g_o is the observed value of gravity reduced to the spheroid and γ_o is the theoretical (normal) gravity value on the spheroid.

The theoretical gravity refers to gravity on the surface of the idealized earth, spheroid, so it is necessary to reduce each data point on the physical surface of earth to the spheroid in computing anomalies associated with it.

In general, the gravity anomaly on the spheroid may be given as:

$$\Delta g = g_h + 0.3086\ h - 0.04191\ \rho h + dg_T - \gamma_o(\phi) \qquad (3.33)$$

where g_h is the observed gravity on the physical surface of the earth, is the station height in meters, ρ is the density of the Bouguer slab in g/cm^3 and dg_T is the terrain correction

3.1 Gravity Measurements

During September - October, 1982 and April 1983, about 400 new gravity stations were occupied in the Central Part of the Main Ethiopian Rift (Lakes District) (Fig. 1.) Measurements were made at 1 to 4 km interval (i.e at 1 km intervals for the Langano - Aluto area and at 2 to 4 km intervals for the rest). Some stations had already been established in this area by Searle and Gouin (1971,1972) along extant roads, tracks and shorelines of lakes. Most of these stations were reoccupied except those along the shorelines to establish a comparison between our Survey and the previous Survey.

Gravity values were measured using the Canadian Sharpe gravimeter no. 128. The scale constant of this meter was found to be 0.10083 mgal/div. This value was determined by standard methods of calibrating a gravimeter.

All the stations occupied in the study area were tied to

the Shashemene USAF gravity base station (977536.42 mgal)

A net of second order gravity base stations were established in the study area being tied to the above mentioned main station. The gravity values were corrected for drift by reading at one control station (A), occuping a second (B) and reading there and returning to the first (A) thereby forming an A - B - A loop connection in 2 to 3 hrs duration. Occasionaly an intermediate control station C would be observed to improve the drift control and the sequence would be A- C - B - C - A. The drift of the gravimeter was assumed to be linear between control stations.

3.2 Elevation and Coordinates of Gravity Stations

In the Aluto - Langano area, station positions and absolute altitudes were determined by tacheometry. For stations outside of Aluto - Langano area elevations were determined using a single Paulin Surveying microaltimeter. Elevation radings were taken concurrently with each gravity observation. In reducing the barometric data corrections were made for temp temperature and for change in barometric pressure. The latter were obtained by observations at points of known elevation and by assuming that the atmospheric pressure varied linearly with time. The final absolute altitudes were obtained by connecting the differences to the bench marks and trigonometric points established by the Ethiopian Mapping Agency

(EMA) almost everywhere in the study area. The majority of the bench marks and trigonometric points used are accurate to ± 0.5 m so that the elevation control was reasonably good.

An accuracy of ± 0.5 m for the (tacheometric observations) and ± 4 m for the barometric observations which may cause corresponding errors of ± 0.1 and ± 1.2 mgals in the Bouguer anomalies may be guaranteed. Sheets of topographic maps supplied by the EMA at a scale of 1:50,000 were available for the entire part of the survey area. The geographic coordinates, longitudes (λ) and latitudes (ϕ) of the gravity stations were scaled from these maps with an estimated accuracy of ± 200 m (0.1 minutes of arc). This may cause a corresponding error in the Bouguer anomalies of ± 0.15 mgal.

3.3 Reduction of Data to Bouguer Anomalies

A combined free - air and Bouguer corrections corresponding to the conventional density of 2.67 gm/cm^3 for the crustal rocks was applied to reduce the observed gravity to mean sea-level (geoid). Theoretical gravity was calculated using the 1930 international gravity formula on the spheroid. Since it was realized that readings at some stations, particularly in the Aluto area would be affected by terrain, terrain corrections were determined out to 15 km for all the stations with an estimated error of ± 0.4 mgal. The terrain corrections varied between 3 and 9 mgals in the Aluto area and between 0.1 and 1.5 mgal in the rest of the survey area. No

tidal corrections were made for all the stations occupied in the study area.

The Bouguer anomalies were then computed by the formula:

$$B.A = g_o + 0.1967\ h - \gamma_o + dg_T$$

where the term g_o is observed gravity at the station and 0.1967 h represents a correction term, consisting of the free-air effect (0.3086 h) and the Bouguer effect (-0.1119h) = (-0.0419ρh) where the density ρ = 2.67 gm/cm^3 and h is the stations elevation in meters. The term γ_o is the theoretical gravity at the latitude of the station calculated by the 1930 international gravity formula on the spheroid. dg_T is the terrain corrections term.

In summary, the main sources of error in the Bouguer anomaly values are:

a) Calibration error: this is a small uncertainty in the scale constant for converting gravimeter readings to mgal and is not likely to introduce an error greater than ± 0.1 mgal.

b) Error involved in reading the gravimeter at each station is about ± 0.005 mgal.

c) Drift error: uncertainties caused by assuming that the drift of the gravimeter is linear between control stations. This is not expected to exceed ± 0.1 mgal.

d) Use of wrong density in the Bouguer reduction; over most of the survey area, the true density of surface rocks is less than 2.67 gm/cm^3 so that the use of the figure 2.67 over

the areas where less dense surface rocks outcrop could lead to an error in the true Bouguer anomaly at sea level.

e) Incorrect elevations and latitudes of stations; in the Aluto - Langano area where elevation and latitude control is reasonably good, this could give an erroro of ± 0.1 mgal elswhere, it could rise to ± 1.2 mgal locally.

The largest errors in the Bouguer anomalies are caused by errors in the elevations. Errors caused by incorrect latitudes of stations and instrument errors are generally much smaller.

To a first approximation it is believed that the total probable error in the Bouguer anomaly values in the studied area is generally less than ± 2 mgals.

Figure 4 shows a contour map of the simple Bouguer anomalies contoured at 4 mgal intervals in the study area at a scale of 1:250,000. The earlier measurements performed by Searle and Gouin have been icluded to facilitate the contouring and to show the regional field outside the rift.

4.0 Interpretation of the Bouguer anomalies

4.1 The Regional Pattern

The nature of the gravity field across the rift zone in East Africa is now well established. Long-wave length (1000 km) negative Bouguer anomalies over the East African Rift System have been found and interpreted by Girdler et al. (1969) and Girdler and Sowerbutts (1970). They consider this long-wave length negative anomaly to be due to low density astenosphere replacing the lithosphere (upper mantle plus crust). This body of low density material (astenolith) extends under the whole of the East African Plateau and is shallowest beneath the rifts. The expansion of the astenosphere into the lower part of the lithosphere gives a negative density contrast causing the long-wave length negative anomaly. The further expansion of the astenosphere into higher levels of the crust (thinning of the lithosphere accounting for the volcanicity beneath the rift in East Africa) gives a positive density contrast causing the short-wave length positive anomaly beneath the rift.

A preliminary consideration of the Bouguer anomaly map (Fig. 4) over the CPMERV (Lakes District) reveals a general correlation between Bouguer anomalies and height. As the higher ground is approached the Bouguer values decrease. There are also deviations from this relationship for some stations in the rift floor where the Bouguer values do not

correlate with height.

As can be seen from the Bouguer anomaly map (Fig. 4), a central positive anomaly (short wave length) occurs over the rift floor and the axis of this anomaly generally coincides with the rift axis. This central positive anomaly is flanked by two relatively narrow negative anomalies and subsidiary positive anomalies along the margins of the rift. All the central positive anomaly and the flanking negative and positive anomalies situated in the rift floor are further flanked by broad negative anomalies on the rift shoulders. The distribution of the Bouguer anomalies in the CPMERV (Lake District) in this fashion may be considered as a superposition of a narrow positive anomaly on a broader negative one.

The broad negative anomaly may be explained by the fact that the low density astenosphere found in the East African Rift System underlies the Ethiopian and Somali plateau also and maybe the cause of this broad negative anomaly.

The relatively narrow negative anomalies in the rift floor may be explained by the fact that the stations producing these anomalies are situated either over large thickness of lake sediments and rift volcanics or are affected laterally by the light mantle derived material (astenoliths) which underlies the Ethiopian and Somali Plateau. The central positive anomaly could be explained interms of mass excess beneath the rift

floor.

The three profiles (profiles A,B,C in Fig. 7) also reflect this phenomenon which is their essential similarity.

4.2 Separation of the Regional and local Anomalies.

The regional anomaly (a somewhat subjective concept) represents the combined effect of variations in density of the basement rocks. Three constraints were put on the choice of the regional anomaly:

1. The negative anomaly over the rift has a considerably greater width (about 100 km).
2. The regional anomaly is assumed to be relatively smoothly varying.
3. The resultant residual anomaly due to the outcroping rocks such as rhyolites, ignimbrites, tuffs, basalts, etc. is assumed to be zero.

To effect the separation by graphical method, (Searle, 1970 a) four parallel profiles across the region were smoothed. These profiles taken from Fig. 4 were selected at a quarter degree intervals (at lines of latitude $8^{o}00'$, $7^{o}45'$, $7^{o}30'$, $7^{o}15'$) (Figs. 5a-5d) approximately perpendicular to the iso-anomalies of figure 4.

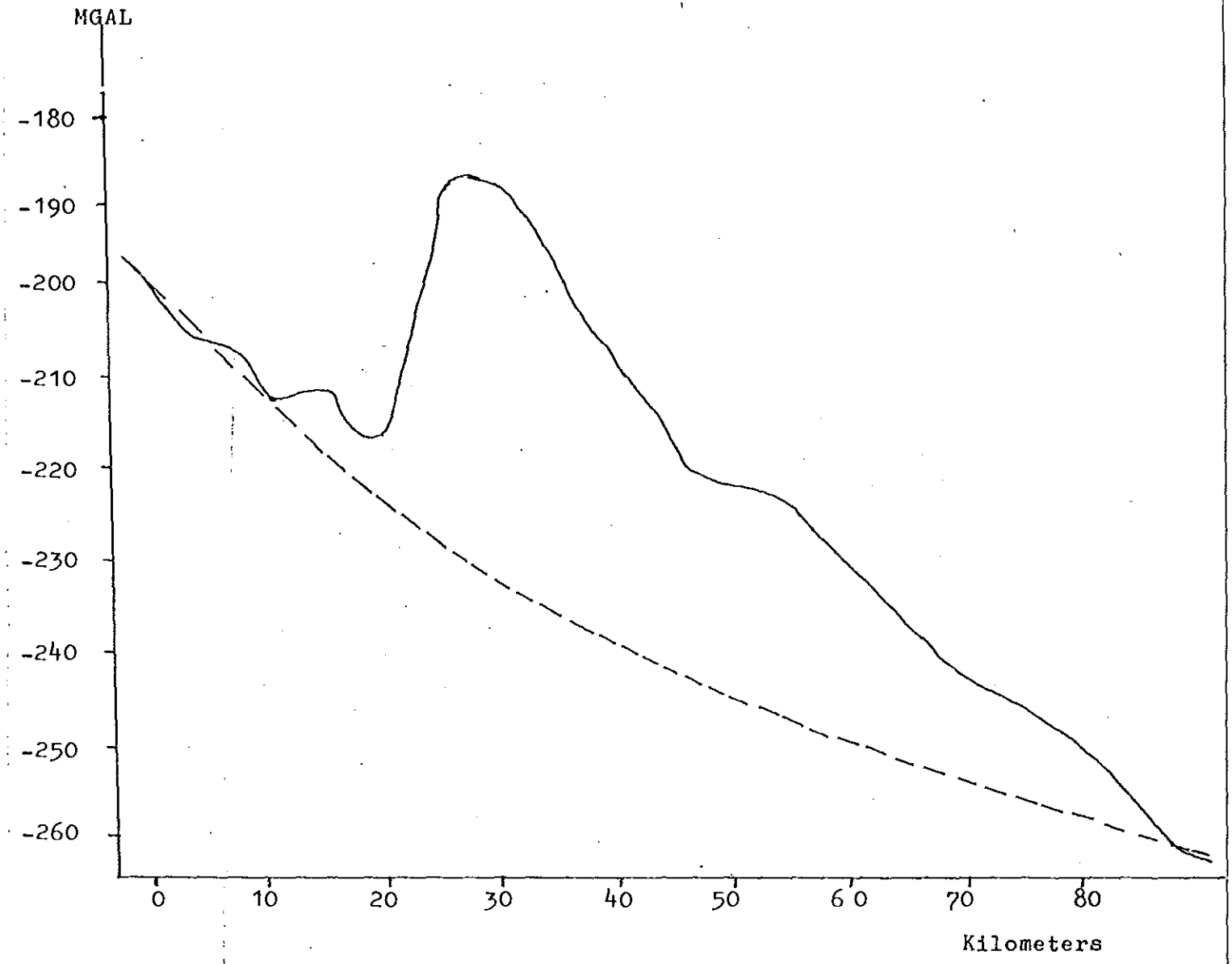

FIG. 5A Profile of Bouguer anomaly along line of latitude 8°00'. Assumed regional anomaly is shown by a broken line.

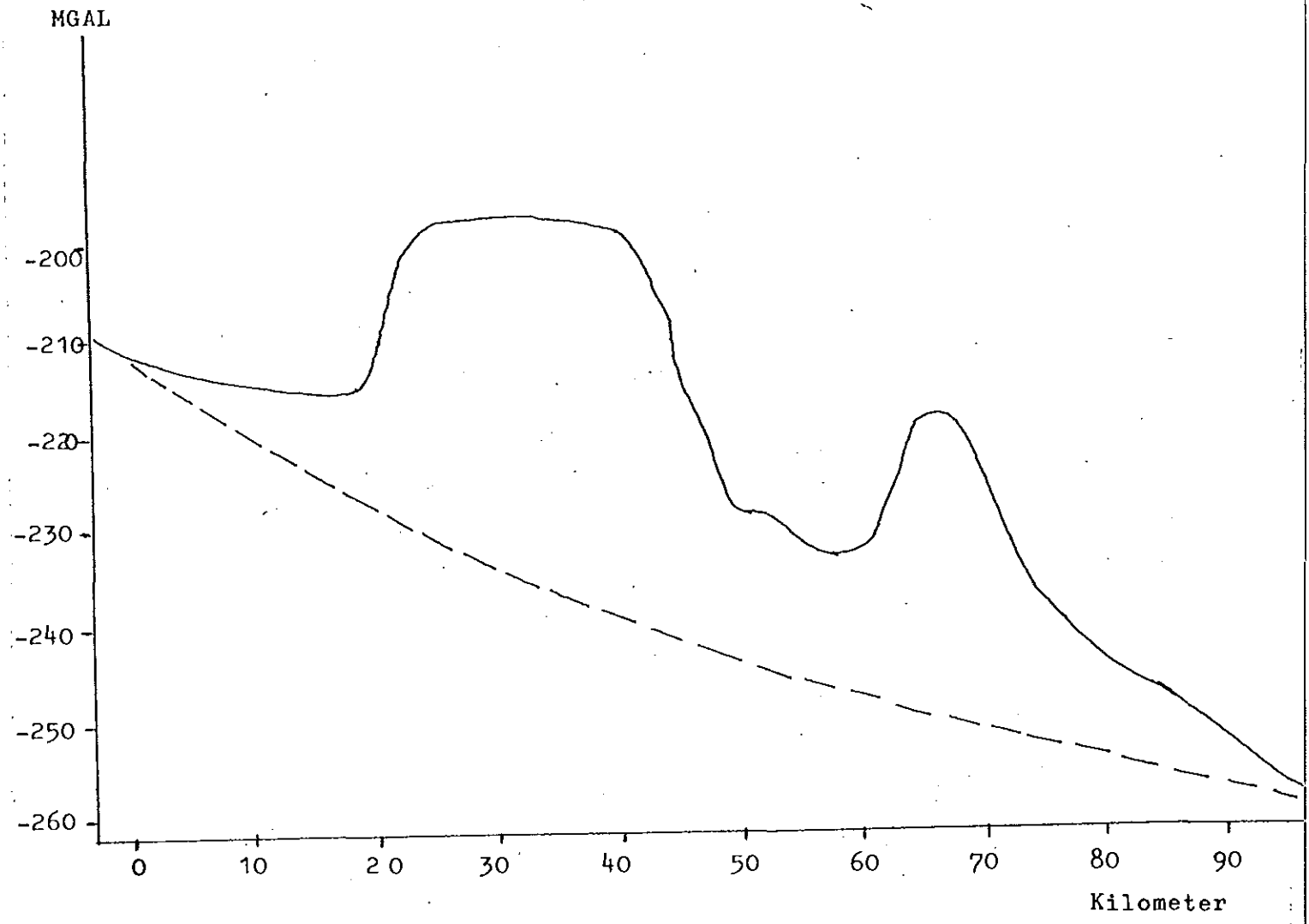

FIG. 5B Profile of Bouguer anomaly along line of latitude 7° 45' . Assumed regional anomaly is shown by a broken line.

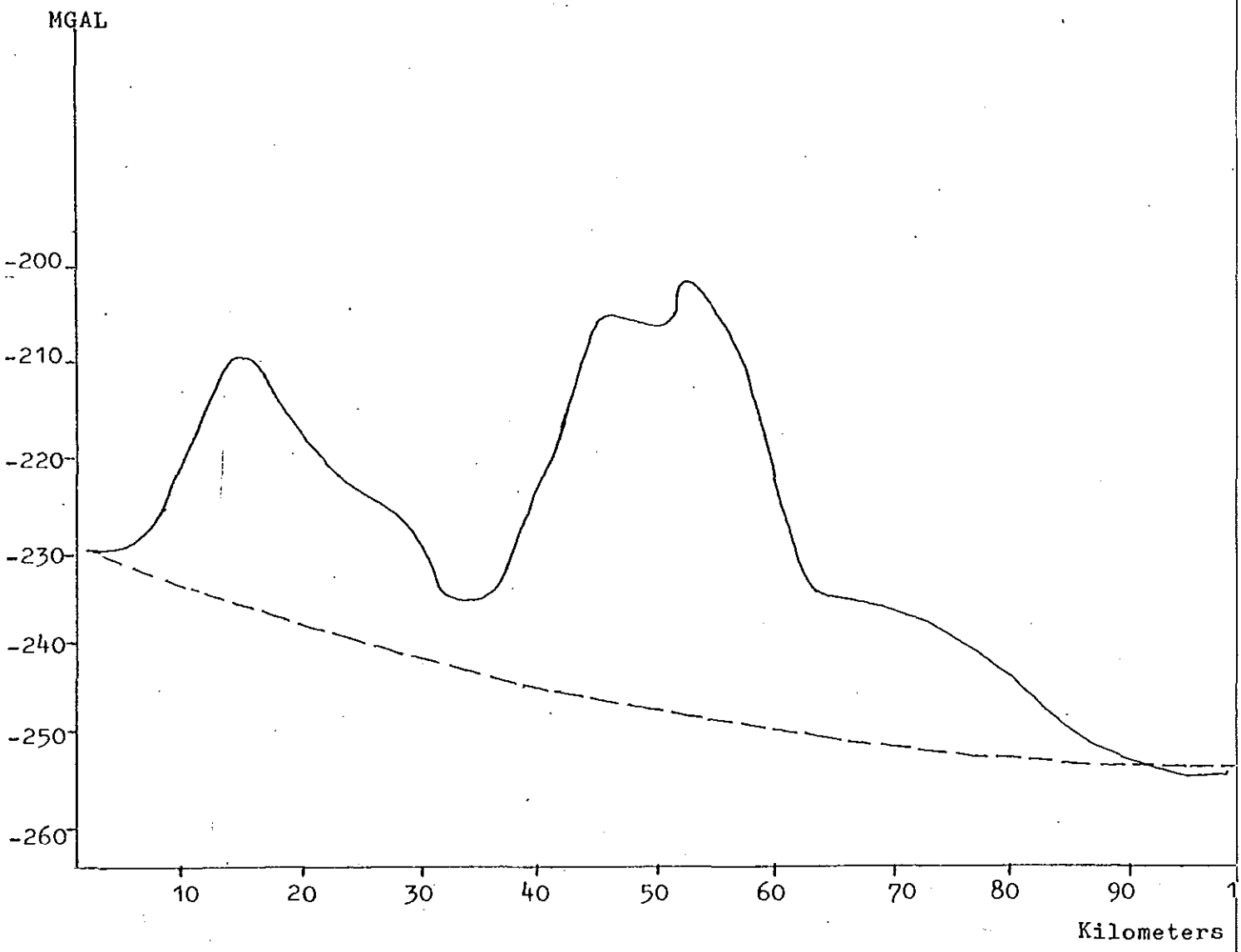

FIG. 5C Profile of Bouguer anomaly along line of latitude $7^{\circ}30'$. Assumed regional anomaly is shown by a broken line.

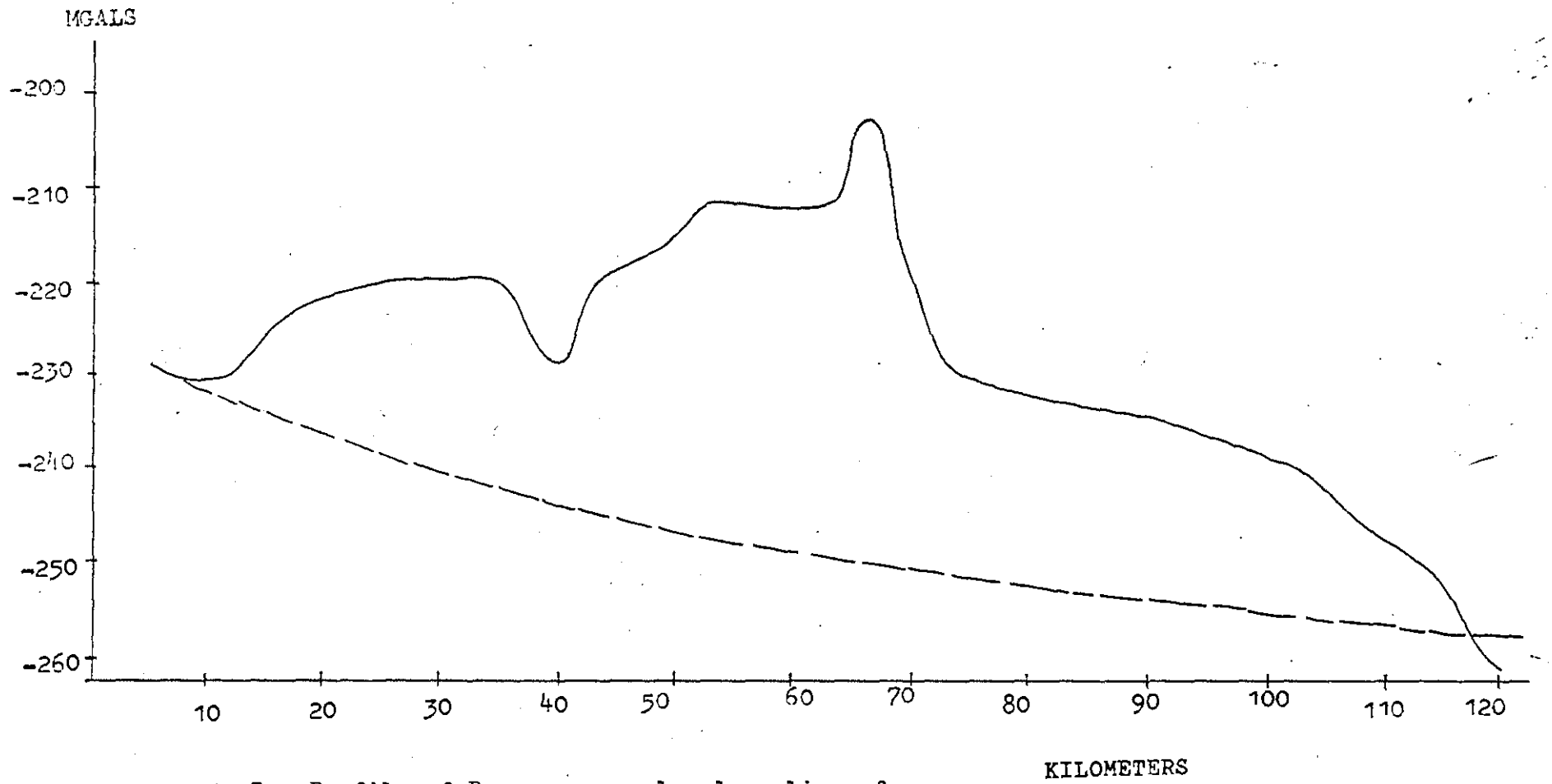

FIG 5D Profile of Bouguer anomaly along line of latitude 7° 15'. Assumed regional anomaly is shown by a broken line.

Bouguer values from these smoothed background curves were plotted on the area map and contoured at 1 mgal intervals. Successive adjustments produced a smooth contoured regional anomaly map (figure 6). The smoothed profiles are shown in figures 5a - 5d. Residual anomalies were then obtained by subtracting the regional anomaly from the observed Bouguer anomaly at each site. The residual anomalies contoured on the area map are shown in figure 7. The residual anomalies (Fig. 7) are similar in outline and trend to the Bouguer anomalies (Fig. 4).

It may be argued that this method is subjective and emperical compared to the analytical methods such as fitting a curve by least squares and second derivative computations and mapping. But in such a survey that covers an area that is smaller than that of a major structural feature governing the regional trends the graphical method, used in this work, has the advantage that all available geological information from the area can be put to use in drawing the regional anomaly. It must also be admitted that this regional anomaly is only approximate because of the isogals of figure 4 intrpolated between widely spaced measurements on the rift shoulders.

5.0 Interpretation of the Positive Bouguer anomalies.

As can readily be seen from the Bouguer anomaly map of figure 4, the relative positive anomalies in the rift floor would generally seem to be situated along the displacement lines of the WFB. The residual anomaly map (Fig. 7) corresponding to the regional gravity field represents the field of these local gravity anomalies that are superimposed on the regional gravity field and reflect the density distribution beneath the rift. The removal of the regional effect leaves a medial area of relatively high Bouguer values in the central zone of the rift floor. Relative positive anomalies which may be considered subsidiary to the medial ones also occur along the margins of the rift.

The medial highs in the CPMERV (Lakes District) culminate in five main positive anomalies, north of Corbetti Caldera near Bura, south west of Shalla Caldera, south of Aluto Caldera and east of Lake Ziway within the WFB and south west of Aluto Caldera near Adami-Tulu outside of the WFB in the central zone of the rift floor. Excepting the Adami-Tulu medial high whose center coincides with rhyolite plugs, all the medial highs mentioned above are associated with the geothermal systems of the Corbetti Caldera, Shalla Caldera, Geyser island situated on a small caldera north of Lake Langano, Aluto Caldera and Tulu-Gudo island within the WFB respectively.

5.1 Interpretation of Profile A

Profile A (Fig. 8) extends north easterly from the positive anomaly on the western margin of the rift ($\phi = 7^{\circ}46'$, $\lambda = 38^{\circ}20'$) across the negative anomaly north of Lake Abiyata. It continues through the broad positive anomaly near Adami-Tulu and the negative anomaly South of Lake Ziway to the enlongated, open and NNE-trending positive anomaly east of Lake Ziway. As mentioned earlier profile A is considered to be typical of the CPMERV (Lake District) in consisting of a central positive anomaly flanked by two negative anomalies and two subsidiary peaks along the margins of the rift. The negative anomalies north of Lake Abiyata and south of Lake Ziway along this profile may be ascribed to maximum thickness of lake sediments and rift volcanics.

A method of estimating the maximum depth to the top of an anomalous mass from gravity anomalies has been derived by Bott & Smith (1959). A special application of this method to the case of a burried step was out lined by Bankroft (1960). It can be seen from figure 8, that the negative anomaly north of Lake Abiyata is bounded to the east and to the west by relatively steep gradients which may be regarded as the effects of two or more burried steps. The expression for the gravitational attraction of such a step is given by Nettleton (1940) and is graphically represented in figure 9.

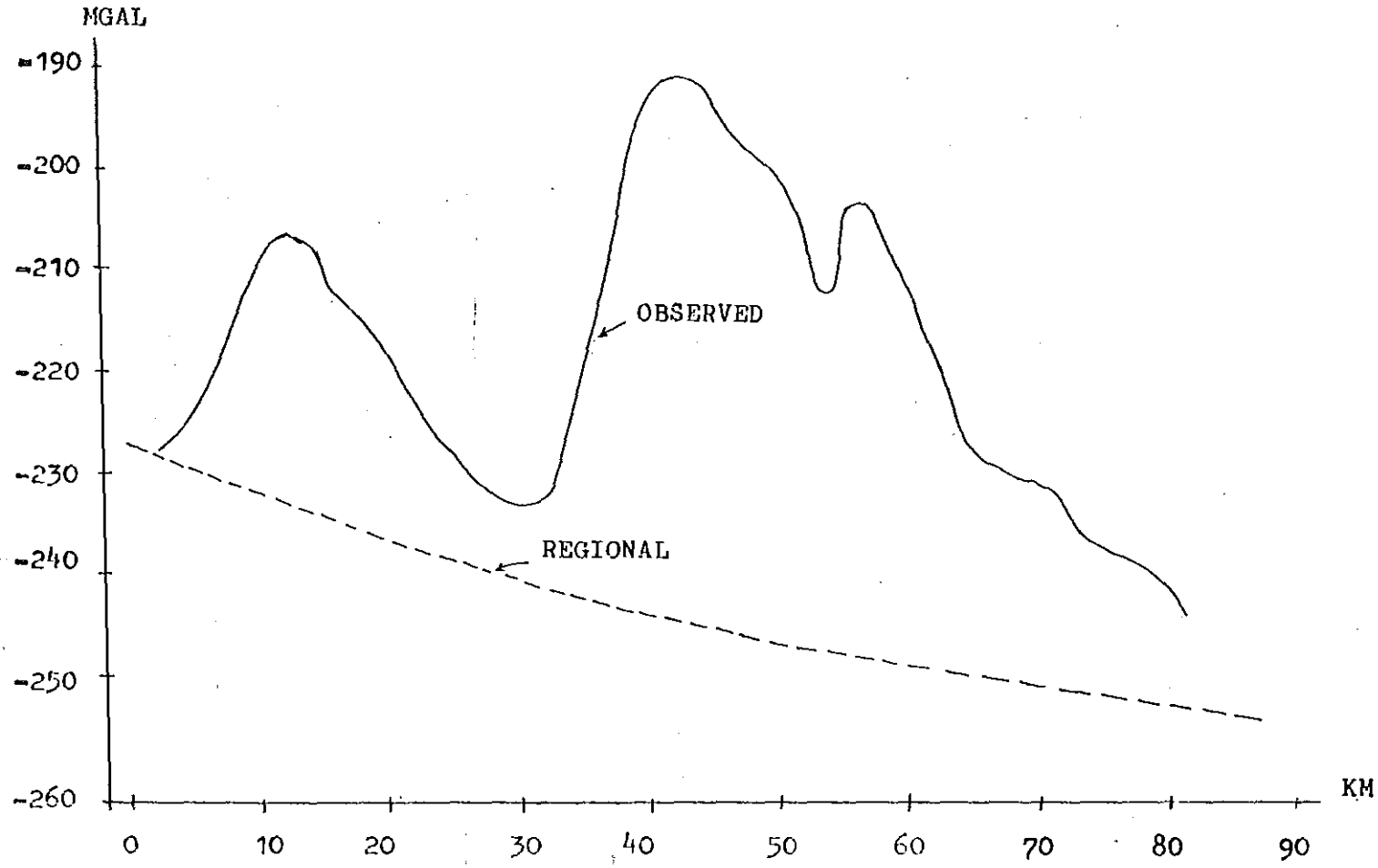

FIG.8 PROFILE A, THE OBSERVED BOUGUER ANOMALY TOGETHER WITH THE DEDUCED REGIONAL ANOMALY

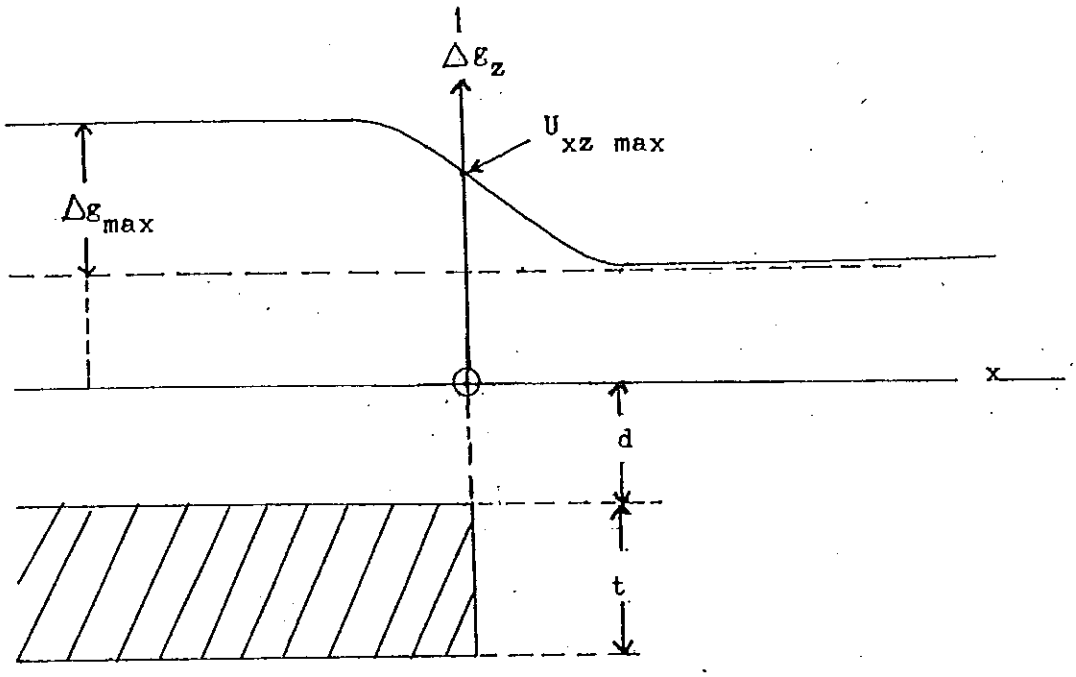

Δg_z = gravity effect of a step

$(U_{xz})_{max}$ = maximum rate of change of Δg_z in x direction

x = horizontal distance perpendicular to step

d = actual depth to top of step

t = thickness of step

Fig. 9. Dimensions and gravity effect of a burried step, after Nettleton (1940).

Bott and Smith give the following formulas for 3 - dimensional and 2-dimensional anomalous masses, respectively.

$$d_o = \frac{0.86\ \Delta g\ max}{U_{xz\ max}} \qquad (5.1)$$

$$d_o = 0.65\ \frac{\Delta g\ max}{U_{xz\ max}} \qquad (5.2)$$

where d_o is the maximum possible depth to the top of the anomalous body, Δg max is the maximum gravity anomaly and $U_{xz\ max}$ is the maximum horizontal gradient of gravity. In the case of a stepped anomaly Bankroft gives

$$d_o = \frac{1}{\pi}\ \left(\frac{\Delta g\ max}{U_{xz\ max}}\right) \qquad (5.3)$$

where d_o is the maximum possible depth of the step, Δg max is the maximum gravity anomaly and $U_{xz\ max}$ is the maximum horizontal gradient of gravity also

$$d = \frac{t}{\ln(1 + t/d)} \qquad (5.4)$$

and $U_{xz} = 2G\ \Delta\rho\ \ln(1 + t/d)$ (5.5)

where d is the actual depth to the top of the step, t being the thickness of the burried step which is found from the formula of an infinite slab:

$$t = \frac{\Delta g\ max}{2\pi\ G\Delta\rho} \qquad (5.6)$$

$\Delta\rho$ is the density contrast and G is the gravitational constant. From equation 4, it can be seen that, as t decreases to very small values, d increases and tends to the value d_o. The maximum depth to the step is therefore d_o. The actual depth,

d is likely to be considerably less than d_o for resonable values of $\Delta\rho$.

The steep gravity gradient with a NNE trend forming the eastern boundary of the Lake Abiyata negative anomaly (Fig. 8) yields the following values:

$$\Delta g \text{ max} = 44.5 \text{ mgal}$$

$$U_{xz \text{ max}} = 5 \text{ mgal/km or } 0.005 \text{ mgal/m}$$

and hence the maximum depth to the step from the above information, substituted in equation (3), gives $d_o = 2.8$ km. The thickness of the step (t) is found by assuming a density contrast of $0.10 gm/cm^3$ between the anomalous body and the surrounding rocks to be t = 10.6 km. With this value the actual depth can be found to be d = 0.25 km.

Near the northern shore of lake Abiyata 0.165 km of sediments were drilled (by Ministry of Mines) but the base was not penetrated. The maximum thickness of sediments found from temperature gradient wells and deep exploratory wells in the Aluto Langano Geothermal prospect area is between 0.2 and 0.26 km. Assuming a density contrast of $-0.7 g/cm^3$ Searle and Gouin (1972), from their gravity data, calculated that the sediment north of lake Abiyata has a maximum thickness of 0.58 km.

The sediment thickness from drilling data seems to be of the same order of magnitude as that determined for the actual

depth of the anomaly causing body, 0.25 km, and hence the thickness of the cover.

The limitation of these rules is that the density contrast of the anomalous body with its surroundings must be entirely positive or entirely negative. This condition is met if it is assumed that there is mass excess in the lower part of the crust beneath the rift floor.

5.2 Models

For the calculations of the gravity anomelies produced by the models to be described, a computer method (written by Caldwell) based on two-dimensional mass distribution (Hubbert, 1948; Talwani et al.1959; Qureshi and Mula, 1971) was employed.

Because of the axial tendency of the WFB within the rift margin envelope and the linear nature of the relative positive anomaly along lines of displacements of the WFB in the rift floor, the two-dimensional representation assumed may be justified here. The model calculations that will be considered below were made for the same profile A taken from the contoured values of the residual anomaly map (Fig. 7).

The central positive anomaly along profile A may be produced by the following models each of which would occupy the central 20-30 km width of the rift floor.

1. A block of high density basement occuring at a depth which can be varied between 2.8 km and an extremly shallow one.
2. Extensive basalt lava flows interbeded with lacustrine sediments and rift volcanics.
3. A zone of intrusives which could occur predominantly within (a) a shallow basement (b) deeper in the Sialic crust.

The following geological evidences are cited for the interpretation of the proposed models.

Lithostratigraphic results from deep exploratory wells sunk on the southern, and SW flanks and on top of the Aluto Caldera by the Aluto-Langano Geothermal prospect give the following valuable geological information. The results are presented diagramatically in figures 10 and 11.

The coordinates, altitudes and observed depths of interfaces between lake sediments plus Aluto Volcanics (ignimbrites, tuffs, rhyolites, etc.) and deep lying basalts from the deep wells are listed in table 1 below.

Table 1.

Well	LA.1	LA.2	LA.3
Longitude	$38^{o}45.8'$	$38^{o}43.6'$	$38^{o}47.6'$
Latitude	$7^{o}43.5'$	$7^{o}47.9'$	$7^{o}47.4'$
Altitude (m)	1601.2	1723.0	1943.4
Interface (m)	261	736	723

As regards the proposed models, neither the existing well data nor surface manifestations generally give evidence to suggest the presence of high density basement rocks in the rift floor. Therefore model 1 is discarded. Model 2 is also thought to be less likely than model 3 although the Shalla Central positive anomaly and the Bura Central positive anomaly may be partly caused by basalt flows which are commonly seen to the south of Shalla Caldera along the Corbetti-Shalla segment of the WFB.

Priliminary models considered in this work are therefore restricted to type 3 (intrusive models).

In figures 12a and 12b are shown two priliminary models (models A and B of type 3) corresponding to two possibilites in which the Central positive anomaly beneath the rift is caused entirely by a zone of intrusives. In model A, the excess mass is assumed to be contained as intermediate

Fig. 10. Geological Sections & Geoelectrical Layerings of

LA - 1 & LA - 2

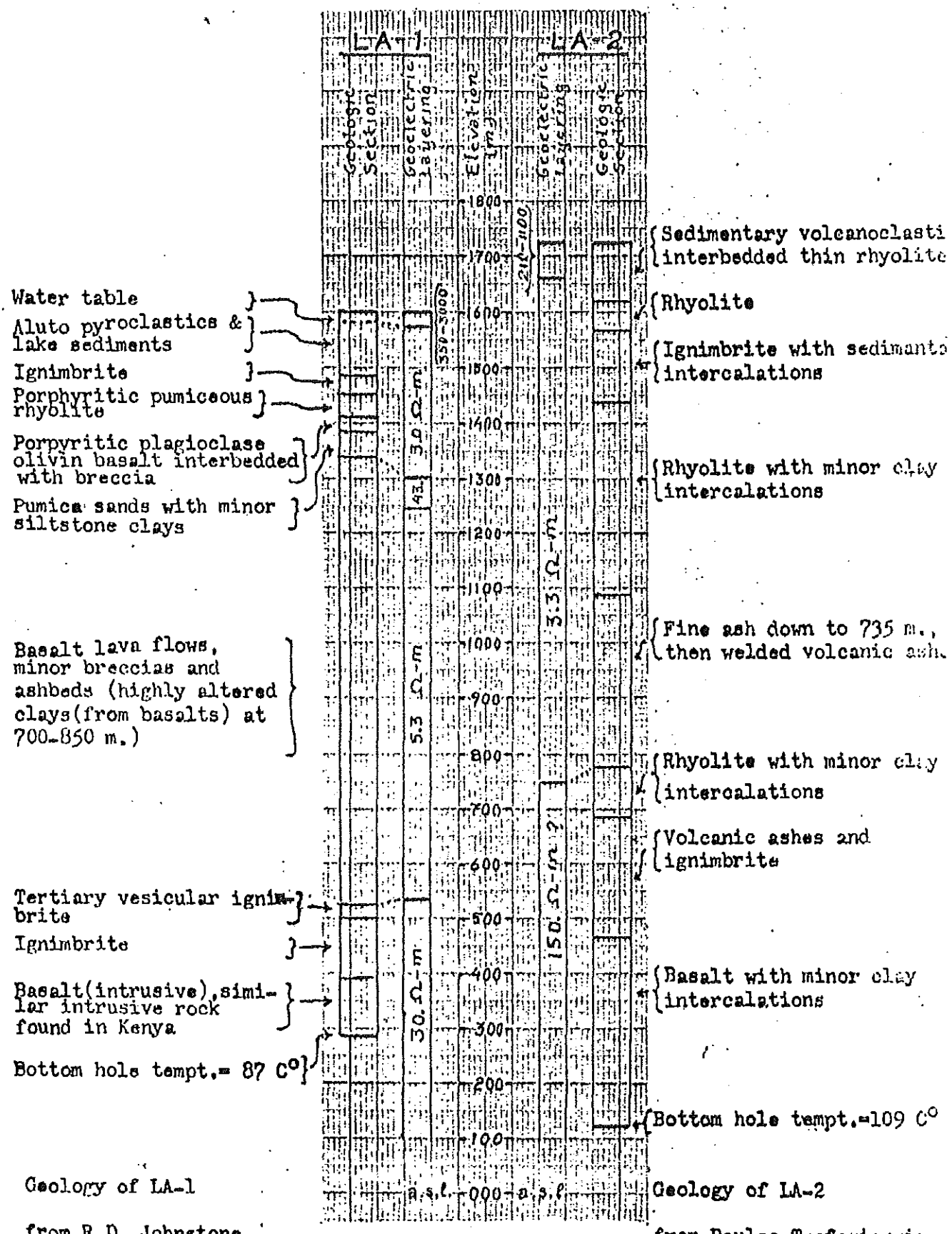

Geology of LA-1

from R.D. Johnstone

Geology of LA-2

from Paulos Tesfagiorgis

Fig. 11. Geological Section & Geoelectrical Layerings
of

LA - 3

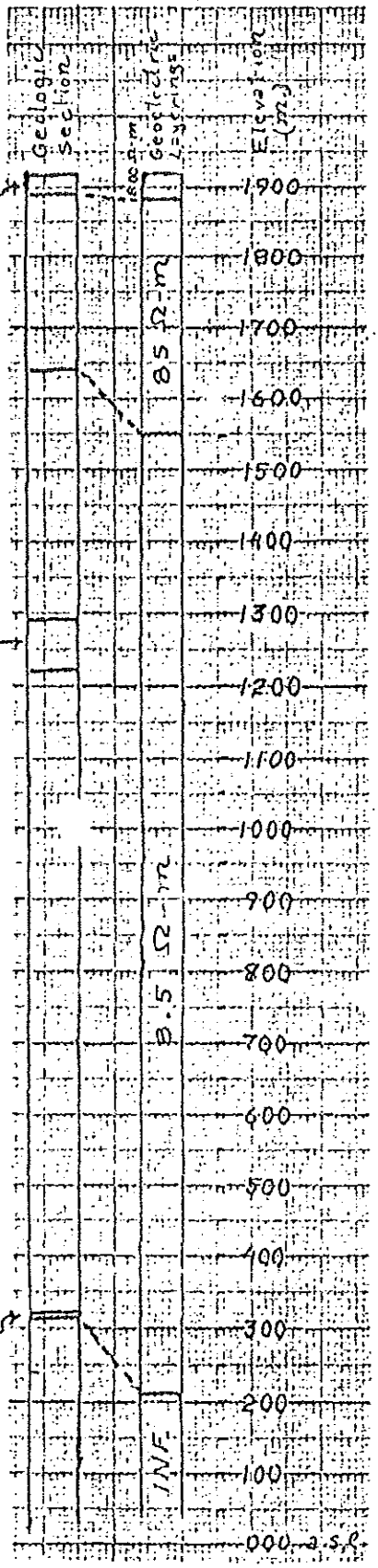

Polymict breccias (pumice, obsidian and rhyolite fragments) with minor ash beds

Rhyolite lava flows with minor ash, sand and silt beds

Light grey to green consolidated silicic breccias and tuffs

Muddy siltstone beds with glas v rhyolite lavas? (interbedded anc probanly rhyolite and pumice breccias also)

Fine grained and some mildly porphyritic basalt lavas, breccias and ash beds with some waterlain ash beds between 1650m-1675m.

Fine grey ash possibly representing the vesicular ignimbrite (5 m thick)

1700m- present depth 1780m. Crystal tuff, ignimbrite, highly welded very rich quartz and totally altered felspar crystals

Geology
from Roy Johnstone & Mareshet Yimer

intrusions (density 2.74 g/cm^3) within the basement while the lake sediments and rift volcanics are assigned a density of 2.63 g/cm^3 so that the density contrast of the intrusive body would be +0.11 g/cm^3. In model B, the base of the intrusive body is put at 16 km and assumed to be dense (density 2.9 g/cm^3) so that it would have a density contrast of +0.23 g/cm^3 with respect to the surrounding sialic crust (density 2.67 g/cm^3). In support of model A, the lithostratigraphic results of the deep wells considered earlier may be cited. The density contrast assumed for these models is inferred from the density measurements on surface samples and cores from production wells of the Olkaria Geothermal Field in Kenya (Hochstein, 1982) (Table 2).

From the generally similar characteristics of the Ethiopian and Kenya rifts as forming the East African rift system and the similar gravity anomalies observed and similar intrusive rocks found (LA.1 result) in both rifts the density values inferred may be justified here.

Shallow model (model A)

With the assumptions made above, model A, was computed. The model showed that the density contrast considered, +0.11 g/cm^3 (2.74 - 2.63), for the intrusive body does not give a Bouguer anomaly which fits the observed profile. If the computed anomalies were to fit the observed profile, then the

TABLE 2 : Densities and porosities of rocks from the Olkaria Geothermal Field (Kenya)

Rock type (Well No.)	Depth (m)	c_d (10^3kg/m^3)	c_w (10^3kg/m^3)	c_p (10^3kg/m^3)	mean %	n
trachyte	surface	<u>2.53</u>[1]	<u>2.56</u>	2.61	3	4
commendite	surface	<u>1.95</u>	2.17	2.50	21	4
(tuffs (ignimbrite (rhyolite	surface	2.18	2.29	2.46	12	3
obsidian	surface	n.d	n.d	n.d	n.d	0
lake sediments	surface	1.78	2.04	2.44	26	1
basalt (core OLK 17)[2]	(240;550)	2.33	<u>2.46</u>	2.68	13	2
basalt (cuttings, OLK 14,15)	(490-575)	n.d	n.d	2.78	n.d	3
rhyolite (core, OLK 16)	(735;740)	2.54	<u>2.58</u>	2.64	4	2
tuffs, rhyolite (cuttings, OLK 4,5,13)	(850-1000)	n.d	n.d	.60	n.d	4
trachyte (core, OLK 16,17)	(1180;1235)	2.38	<u>2.50</u>	2.70	12	2
trachyte (cuttings, OLK 6,14,16)	(1000-1600)	n.d	n.d	2.66	n.d	4

Note: [1] Standard deviation of density values for samples with n 2 all lie between 0.04 and 0.09x10^3kg/m^3; best representative values of gross densities are underlined.

[2] Number of well from which cuttings and cores were taken.

Explanation of columns and remarks:

c_d = dry density (sample dried for 48 hr at 105°C; dry mass of most samples 250 g);

c_w = wet density (sample saturated under vacuum of 0.2 bar for 48 hr);

c_p = particle density (computed for cores and surface samples, measured for cuttings using the pykometer method);

= porosity (computed);

n = total number of samples;

n.d = not determined.

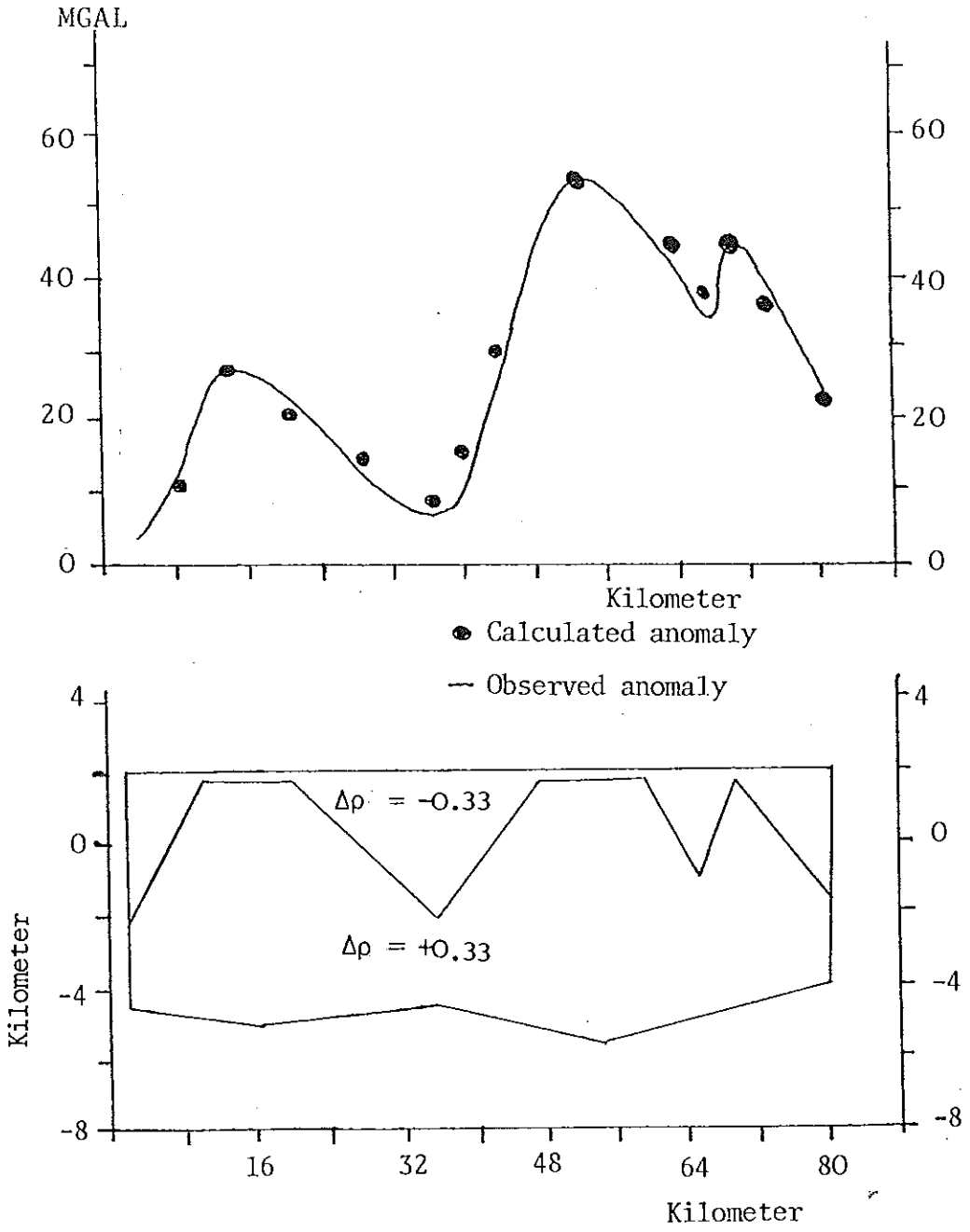

FIG. 12A. Model A: Residual Bouguer anomalies with an intrusive model computed assuming a mass excess confined to a shallow basement

density contrast of the intrusive body should be greater than or equal to + 0.33 g/cm^3 with the surrounding rocks and its upper surface coincident with the land surface at places (Fig. 12 a). From a consideration of the available bore hole data and surface geology, it is unlikely that material in the rift floor can have such a high density contrast. This value, +0.33 g/cm^3, therefore represents an upper limit for the density contrast of the intrusive body. From the above given arguments, it is concluded that it is impossible to account for all of the positive anomaly by means of dense intrusives confined within a shallow basement on the rift floor.

Deep model (model B)

If the observed Bouguer anomaly is not the result of dense intrusives confined within a shallow basement in the rift floor, the only reasonable alternative seems to be high standing (deep reaching) crustal intrusions of astenospheric material (astenolith) or other igneous rocks derived from the astenosphere.

Model B (Fig. 12 b) has been computed on the assumption that the lake sediments and rift volcanics have a density contrast of -0.17 (2.50 - 2.67) g/cm^3 while a density contrast of +0.2 is assigned for the intrusive body. The depth to the base of the intrusive body is taken at 16 km. The computed anomalies fit the observed one to within 2 mgals everywhere,

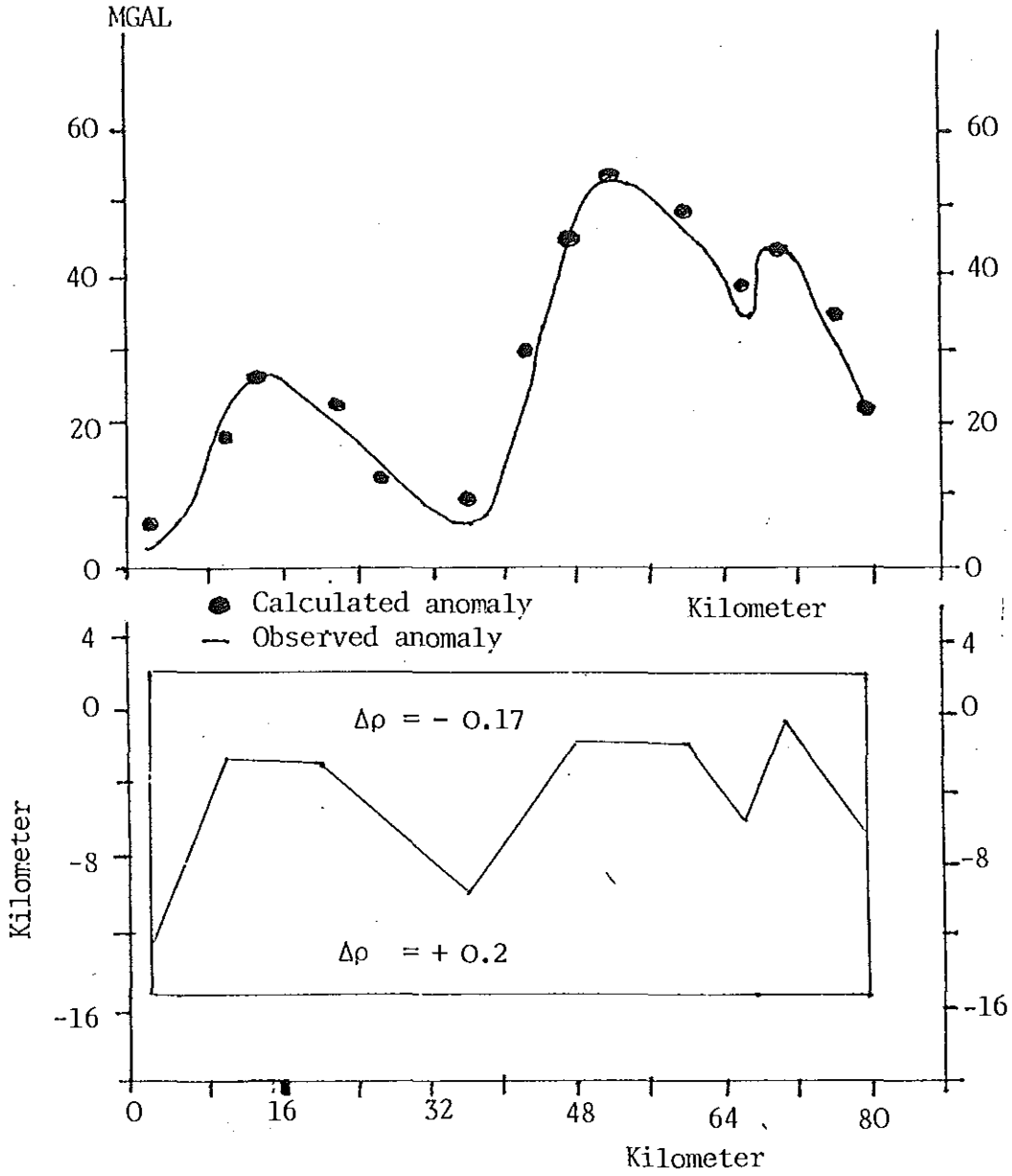

FIG. 12B. Model B: Residual Bouguer anomalies with an intrusive model computed assuming a mass excess confined in the sialic crust. A density contrast of -0.17 for the lake sediments plus rift volcanics and +0.2 for the intrusive body with respect to the crustal density was used.

the intrusive body reaching to within 2 - 3 km of the surface at places. The model (Fig. 12 b) also indicates that there are three zones of intrusion, a central zone along the axis of the rift floor and two subsidiary zones along the margins of the rift. A similar feature occurs in the Kenya Rift, although the magnitude varies (Searle, 1970).

The association of geothermal manifestations, Quaternary Volcanic Centers (Corbetti Volcanic Center, Shalla Volcanic Center, Gademota Caldera and Aluto Volcanic Center) and recent faultings (WFB) with the central positive anomaly in the CPMERV could support the model of deep reaching crustal intrusions of astenospheric material over the whole width of the rift as model B suggests.

5.3 Comparison with adjacent areas

Makris et al. (1969, 1970) have published a paper on crustal and upper mantle models from gravity measurements across the Ethiopian Rift between latitudes of 8°N and 9°N. These models show a thinning of the crustal layers and an intrusion of upper mantle material beneath the rift.

There is a fair agreement with the concept that, north to south, in Ethiopia, we proceed from the oceanic crust of the central Red Sea graben to the major crustal thinning with some oceanic crust at Erta Ale in the Afar (Makris, 1972) to the WFB the axis of the Main Ethiopian Rift. The gravity

anomaly associated with these features decreases from the Red Sea through Afar to the CPMERV (Fig. 13).

The development of the positive gravity anomaly seems to be dependent on the extent to which the axial intrusive has developed. Over the Gulf of Aden and Red Sea, the positive anomaly is much more pronounced and here the intrusive zones are correspondingly larger.

Further south, in Ethiopia, the axis of the rift is transferred to the Margariata, Stephane, Rudolf, and finally to the Gregory rifts. The Rudolf axis has a major positive anomaly with values comparable to the Afar area. In contrast to the Rudolf positive anomaly the Gregory Rift has a broad negative anomaly with a minor axial positive anomaly indicative of mafic intrusions (Searle, 1970; Darracott et al., 1972).

On the basis of the axial gravity highs as indicative of the development of axial intrusives, the CPMERV might be viewed as intermediate to the Rudolf - Margariata rifts and the Afar region.

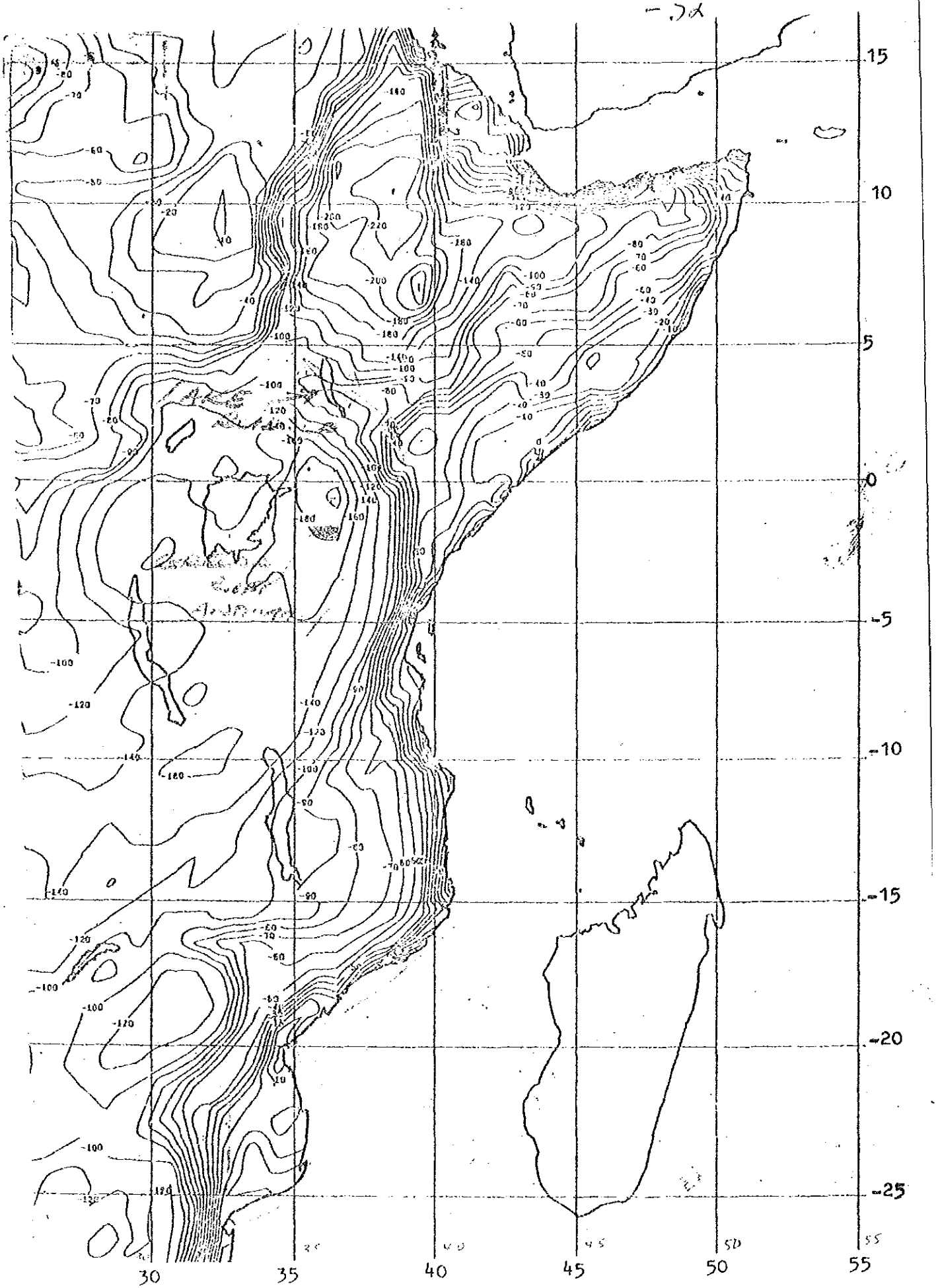

Fig. 13 NASA Gravity Map of Africe

6.0 Summary and Conclusions.

The Bouguer anomalies of the CPMERV have been interpreted interms of varying geological conditions. Profile A has been taken as representative of the rift floor and two models (Fig. 12 A,B) which reasonably fit this profile have been discussed.

Without doubt further refinements of the observations, and consequently of the interpretations, can be made.

Additional geophysical work such as seismic, together with more detailed studies of the gravity field will provide better data for quantitative interpretations.

Further geological work will also be necessary to provide an improved version of the present work. In addition much density information is needed for the whole area.

The main features of the results obtained in this work can be summarized as follows:

1. Within the rift floor, a central zone of positive anomaly is flanked, over most of the studied area, by negative anomalies. These negative anomalies could be ascribed to maximum depths of Lake sediments and rift volcanics confined to two relatively narrow troughs.
2. The crust is thinner beneath the central zone than under the flanking basements and this would correspond to a zone of high density intrusives. The centers of this intrusives

are at Bura, Shalla, Northern Langano, and Adami-Tulu.

3. The central positive anomaly is associated with the axial zones of recent faulting (WFB), volcanism and geothermal activity.
4. The present work shows that the Aluto Volcanic Complex is associated with positive anomaly rather than negative anomaly as suggested Searle and Gouin (1972) and this positive anomaly extends NNE following the Wonji Fault Belt.
5. There is little or no dependence of the positive Bouguer anomalies on elevation beneath the rift floor.
6. Based on currently available bore hole data figures 10 and 11, the lake sediments beneath the rift floor do not appear to have much effect on the gravity field.
7. The models generated clearly show that the positive gravity anomalies are controlled by intrusives and the contribution of lake sediments and rift volcanics is relatively negligible.

7. REFERENCE

Baker, B.H. and Mitchell, J.G., 1976. Volcanic Stratigraphy and Geochronology of the Kedong - Olorgesaile Area & the Evolution of the South Kenya Rift Valley. J. Geol. Soc. London 132: 467-484.

Bankroft, A.M., 1960. Gravity anomalies over a buried step. J. Geophys. Res. 65: 1630-1631.

Bott, M.H.P., & Smith R.A., 1958. The Estimation of the Limiting Depth of Gravitating Bodies. Geophys. Prosp. 6: 1-10.

Garland, G.D., 1979. Introduction to Geophysiscs - Mantle, Core and Crust. W.B. Saunders Company 134-177.

Girdler, R.W., 1958. The Relationship of the Red Sea to East Africa Rift System. Q.J. Geol. Soc-Land., 114: 79-105.

Girdler, R.W., Fairhead, J.D., Searle, R.C. & Sowerbutts, W.T.C., 1969. The Evolution of Rifting in Africa, Nature, 224 1178-1182.

Girdler, R.W., & Sowerbutts, W.T.C., 1970. Some Recent Geophysical Studies of the Rift System in East Africa - J. Geomagn. Geoelectr., 22: 153-163.

Gouin, P., & Mohr, P.A., 1964. Gravity Traverses in Ethiopia (intrimreport) Bull. Geophys. Obs. Addis Abeba, 7: 185-239.

Hubbert, M.K., 1948. A Line-integral method of computing the Gravimetric Effects of Two-dimensional Masses. Geophys. 13: 215-225.

Lloyd, E.F., 1977. Geological Factors Influencing Geothermal Exploration in the Langano Region, Ethiopia. Privately Circulated Report, 73pp.

Makris, J., Menzel, H., Zimmermann, J., Bonjer, K.P., Fuchs, K. & Wohlenberg, J., 1969. Crustal & Upper-Mantle Structure of the Ethiopian Rift Derived from Seismic & Gravity Data. Z. Geophys. 36: 387-391.

Makris, J. Thiele, P. & Zimmermann, J., 1970. Crustal Investigation from Gravity Measurements at the Scrap of the Ethiopian Plateau. Zeitschr. Geophys., 36: 299-311.

Mohr, P.A., 1960. Report on a Geological Excursion through Southern Ethiopia. Bull. Geophys. Obs. Addis Abeba 3: 9 - 20.

___, 1962. The Ethiopian Rift System, Bull. Geophys. Obs. Addis Abeba, 5: 33-62.

___, 1966a. Chabbi Volcano (Ethiopia) Bull. Volcanol. 29:797-816.

___, 1966b. Geological Report on the Lake Langano & Adjacent Plateau Regions. Bull. Geophys. Obs. Addis Abeba, 9:59-75.

___, 1967. The Ethiopian Rift System. Bull. Geophys. Obs., Addis Abeba, 11: 1-65.

___, Mitchell, J.G., Raynolds, R.G.H., 1980. Quaternary Volcanism & Faulting at O'A Caldera, Central Ethiopian Rift. Bull. Volcanol.,43 : 173 - 189.

Nettleton, L.L., 1940. Geophysical Prospecting for oil McGraw-Hill, 444P.

Qureshi, I.R. & Mula, H.G., 1971. Two-dimensional Mass Distributions from Gravity Anomalies: a Computer method Geophys. Prospect. 19; in press.

Searle, R.C., Gouin, P., 1970. Evidence of Gravity anomalies for the Thinning of the Lithosphere Beneath the Rift Valley in Kenya. Geophys. Journal Roy. Astron. Society. 21: 13-30.

___, 1972. A Gravity Survey of the Central Part of The Ethiopian Rift Valley Tectonophysics. 15: 41-52.

___, 1972. Local Earthquake Phases Observed at Addis Abeba, Ethiopia. In: R.W. Girdler (Editor), East African Rifts. Tectonophysics, 15: 55-57.

Talwani, M., Worzel, J.L. & Landisman, M., 1959. Rapid gravity computations for Two-dimensional Bodies with Application to the Mendacino Submarine fracture zone, J. Geophys. Res., 64: 49-59.

APPENDIX I

PRINCIPAL FACTS FOR GRAVITY STATIONS

No. 1 - 242 - Class A

No. 243 - 402 Class B

Other gravity stations occupied by Searle and Gouin are classed as C.

No	Station	Altitude (m)	Longitude (deg. min)	Latitude (deg.min)	G.obs. (mgal)	F.A (mgal)	Sg_T (mgal)	B.A (mgal)
1	14/-0.15	1637.5	38 44.8	7 53.8	616.38	-24.54	0.12	-207.65
2	14/0.2	1636.6	38 44.8	7 53.7	617.12	-23.86	0.20	-206.79
3	14/2.0	1644.25	38 44.6	7 52.8	622.54	-15.83	0.25	-199.57
4	BM_{95}	1646.70	38 44.4	7 51.8	619.67	-17.54	0.28	-201.53
5	BM_{94}	1658.75	38 44.5	7 52.2	618.28	-15.36	0.31	-200.67
6	14/5.0	1650.69	38 44.2	7 51.1	619.00	-16.62	0.6	-200.54
7	14/6.0	1666.49	38 44.1	7 50.6	615.91	-14.71	0.8	-200.4
8	14/7.0	1677.90	38 44.0	7 50.0	615.58	-11.31	0.44	-198.63
9	14/8.0	1675.52	38 43.9	7 49.5	615.67	-11.64	0.86	-198.38
10	14/9.0	1687.82	38 43.8	7 49.0	613.61	- 9.8	1.02	-197.65
11	14/9.9	1712.46	38 43.7	7 48.5	605.52	-10.09	1.18	-200.54
12	14/11.0	1723.00	38 43.6	7 47.9	602.81	-9.32	1.13	-201.00
13	14/12.0	1727.36	38 43.5	7 47.4	605.30	-5.28	1.60	-197.15
14	14/13.0	1706.24	38 43.4	7 46.9	604.78	-12.10	1.48	-201.56
15	14/14.0	1689.94	38 43.2	7 46.4	610.35	-11.35	1.37	-199.09
16	14/15.0	1664.69	38 43.1	7 45.8	613.48	-15.81	1.00	-201.09
17	14/16.0	1647.69	38 42.9	7 45.3	617.31	-17.01	0.64	-200.75
18	14/17.0	1631.92	38 42.9	7 44.8	619.49	-19.50	0.42	-201.69
19	14/18.0	1613.11	38 42.8	7 44.3	619.80	-24.78	0.2	-205.09
20	14/19.0	1605.50	38 42.7	7 43.8	619.34	-27.38	0.4	-206.64
21	14/20.0	1600.62	38 42.6	7 43.2	618.25	-29.77	0.31	-208.57
22	14/21.0	1596.75	38 42.5	7 42.7	617.23	-31.76	0.25	-210.21
23	14/22.0	1591.71	38 42.4	7 42.2	616.85	-33.51	0.2	-211.42
24	14/23.0	1588.15	38 42.2	7 41.6	615.73	-35.48	0.2	-212.99

No	Station	Altitude (m)	Longitude (deg .min)		Latitude (deg. min)		G.obs. (mgal)	F.A (mgal)	Sg_T (mgal)	B.A (mgal)
25	14/24.0	1585.62	38	42.1	7	41.0	615.2	-36.57	0.2	-213.8
26	14/25.0	1584.60	38	42.0	7	40.5	615.58	-36.29	0.18	-213.43
27	3N/0.0	1595.79	38	47.3	7	42.8	632.19	-17.14	1.65	-194.06
28	3N/1.0	1596.17	38	46.8	7	43.0	632.04	-17.27	1.55	-194.33
29	3N/2.0	1595.75	38	46.1	7	43.3	631.95	-17.58	1.34	-194.8
30	3N/3.0	1601.2	38	45.8	7	43.5	629.28	-18.66	1.34	-196.49
31	3N/4.0	1618.97	38	45.4	7	43.7	622.25	-20.31	1.41	-200.06
32	3N/5.0	1619.95	38	44.9	7	44.0	619.76	-22.59	1.30	-202.56
33	3N/6.0	1627.73	38	44.4	7	44.2	615.71	-24.33	2.32	-198.15
34	3N/7.0	1627.37	38	43.9	7	44.5	617.69	-22.56	2.34	-202.32
35	3N/8.0	1631.93	38	43.4	7	44.7	619.01	-19.94	1.80	-200.75
36	3N/9.0	1636.45	38	42.9	7	45.0	618.86	-18.78	1.07	-200.83
37	3N/10.0	1635.64	38	42.4	7	45.2	618.73	-19.26	0.73	-201.56
38	14/1W	1663.28	38	42.7	7	46.5	615.68	-14.30	1.37	-199.05
39	14/2W	1654.03	38	42.2	7	46.6	620.64	-12.24	0.76	-196.56
40	14/3W	1656.15	38	41.7	7	46.7	621.14	-11.12	0.42	-196.02
41	14/4W	1657.10	38	41.1	7	46.8	621.13	-10.89	0.36	-195.95
42	E_1	1595.00	38	42.1	7	38.9	610.01	-38.00	0.12	-216.36
43	Bm12	1592.34	38	40.4	7	39.2	609.82	-39.13	0.08	-217.23

No	Dtation	Alt (m)	Longitude (deg. min)	Latitude (deg.min)	Gobs. (mgal)	F.A (mgal)	Sg_T (mgal)	B.A (mgal)
44	Bm_{11}	1589.50	38 40.2	7 40.2	611.12	-39.12	0.09	-216.89
45	Bm_{10}	1588.41	38 39.7	7 40.7	610.39	-40.39	0.10	-218.03
46	Bm_9	1591.63	38 39.5	7 41.4	609.94	-40.12	0.13	-218.1
47	Bm_8	1598.69	38 39.2	7 42.5	608.83	-39.47	0.10	-218.27
48	Bm_7	1601.74	38 39.0	7 43.0	607.62	-39.97	0.11	-219.1
49	Bm_6	1607.73	38 38.6	7 44.1	607.19	-38.98	0.12	-218.77
50	Bm_5	1618.09	38 38.6	7 45.2	609.02	-34.37	0.14	-215.32
51	Bm_4	1629.62	38 38.7	7 45.7	610.01	-30.05	0.14	-212.26
52	Bm_3	1652.61	38 39.3	7 46.7	614.99	-18.36	0.13	-203.16
53	Bm_2	1650.54	38 39.9	7 47.6	623.87	-10.50	0.12	-195.07
54	Bm_1	1653.37	38 40.5	7 48.5	630.25	- 3.59	0.14	-188.46
55	Bm_{49}	1651.83	38 41.0	7 49.3	627.65	-6.99	0.05	-191.77
56	Bm_{50}	1657.17	38 41.6	7 50.3	627.39	- 6.02	0.04	-191.41
57	Bm_{51}	1648.31	38 42.2	7 51.2	622.81	-13.69	0.04	-198.1
58	Bm_{52}	1646.99	38 42.3	7 52.0	622.69	-14.51	0.08	-198.72
59	Bm_{54}	1584.82	38 45.5	7 42.6	637.96	-14.68	0.92	-192.11
60	Bm_{57}	1588.78	38 45.2	7 42.1	635.16	-16.05	1.50	-192.34
61	Bm_{63}	1583.59	38 43.2	7 41.3	619.08	-33.42	0.10	-210.57
62	Bm_{64}	1583.97	38 42.6	7 40.8	615.76	-36.43	0.12	-213.55

No	Station	Alt (m)	Longitude (deg. min)		Latitude (deg. min)		G (mgal)	F.A (mgal)	Sg_T (mgal)	B.A (mgal)
63	Bm_{65}	1584.77	38	42.0	7	40.4	615.48	-36.30	0.10	-213.54
64	Bm_{66}	1588.93	38	41.4	7	41.1	613.66	-37.10	0.1	-214.8
65	Bm_{60}	1592.76	38	40.7	7	41.3	614.21	-35.45	0.09	-213.6
66	E_3	1587.00	38	39.7	7	40.8	610.53	-40.71	0.08	-218.22
67	T_7	1583.00	38	38.7	7	40.6	606.82	-45.58	0.10	-222.62
68	Bm42	1597.46	38	47.3	7	42.8	631.41	-17,39	1.13	-195.02
69	Bm53	1581.44	38	46.4	7	42.8	633.73	-20.03	0.92	-196.07
70	Bm_{55}	1595.18	38	44.6	7	42.9	628.73	-20.85	0.45	-198.9
71	Bm_{56}	1591.58	38	43.5	7	42.8	619.96	-30.68	0.38	-208.4
72	Bm_{29}	1594.94	38	42.5	7	42.8	617.37	-32.21	0.12	-210.56
73	Bm_{28}	1594.64	38	41.5	7	42.6	616.43	-33.17	0.10	-211.52
74	Bm_{27}	1603.89	38	40.4	7	42.7	613.90	-32.91	0.09	-212.29
75	4NS-2.7 / 0.0 E	1634.76	38	46.0	7	43.9	619.19	-18.57	2.6	-198.9
76	4NS-2.7/ 1.00 E	1625.40	38	46.5	7	43.8	622.85	-17.72	1.95	-197.66
77	4NS-2.7/ 2.0 E	1619.61	38	47.0	7	43.6	624.46	-17.83	1.83	-197.23
78	4NS-2.7/ 2.9 E	1629.08	38	47.5	7	43.4	622.41	-16.88	1.85	-197.32

Nº	Station	Alt (m)	Longitude (deg. min)	Latitude (deg. min)	G.obs (mgal)	F.A (mgal)	Sg_T (mgal)	B.A (mgal)
79	4NS-2.7/ 1.0 W	1655.69	38 45.5	7 44.1	615.64	-15.74	2.26	-198.76
80	4NS-2.7/ 2.0 W	1651.55	38 45.0	7 44.3	613.82	-18.92	2.12	-201.61
81	4NS-27 / 3W	1656.96	38 44.5	7 44.5	610.05	-21.10	2.25	-204.26
82	4NS-2.7/ 4.0 W	1643.19	38 44.0	7 44.7	614.37	-21.11	2.04	-202.94
83	4NS-2.7/ 5.0 W	1643.53	38 43.5	7 44.9	617.84	-17.62	1.34	-200.18
84	4NS-3.4/ 0.0	1696.63	38 46.2	7 44.5	605.29	-13.53	2.96	-200.42
85	4NS-3.4/ 0.9 W	1708.06	38 45.7	7 44.5	603.90	-11.46	3.11	-199.48
86	4NS-3.4/ 2.10 W	1706.35	38 45.1	7 44.7	602.04	-13.94	2.95	-201.93
87	4NS-3.4/ 3.0 W	1697.82	38 44.7	7 44.9	602.93	-15.74	2.19	-203.54
88	4NS-3.4/ 4.0 W	1679.78	38 44.2	7 45.1	605.58	-18.74	1.75	-204.95

No	Station	Alt (m)	Longitude (deg. min)		Latitude (deg. min)		G.obs (mgal)	F.A (mgal)	Sg_T (mgal)	B.A (mgal)
89	4NS-3.4/ 5.0 W	1681.06	38	43.7	7	45.2	606.94	-17.05	0.88	-204.28
90	4NS-0.4/ 0.0	1586.02	38	45.6	7	42.8	636.68	-15.65	0.85	-192.27
91	4NS-0.4/ 1E	1582.12	38	46.1	7	42.7	634.45	-19.07	0.93	-195.18
92	4NS-0.4/ 2E	1582.36	38	46.6	7	42.6	631.02	-22.37	0.72	-198.72
93	4NS-0.4/ 3E	1582.83	38	47.2	7	42.5	631.46	-21.77	0.95	-197.93
94	4NS-0.4/ 4.3 E	1700.22	38	47.9	7	42.4	607.45	- 9.51	0.38	-199.39
95	3N-1E/ 1.S	1631.96	38	47.6	7	42.0	628.11	-19.15	0.73	-197.49
96	3N-1E/ 1.9 S	1630.53	38	47.3	7	41.6	623.13	-15.01	0.44	-197.02
97	3N-1E/3 S	1596.05	38	47.1	7	41.1	630.04	-18.53	1.34	-195.78
98	3N-1E/ 3.8 S	1587.61	38	46.9	7	40.7	631.36	-19.65	0.86	-196.45

No	Station	Alt (m)	Longitude (deg. min)		Latitude (deg. min)		G.obs (mgal)	F.A (mgal)	Sg_T (mgal)	B.A (mgal)
99	12/3s	1680.42	38	48.3	7	42.0	610.04	-12.86	0.28	-200.62
100	12/4s	1689.36	38	48.0	7	41.5	609.06	-10.89	0.14	-199.79
101	12/5s	1665.41	38	47.8	7	41.1	613.99	-13.16	0.12	-199.4
102	12/6s	1630.70	38	47.6	7	40.6	620.92	-16.75	0.33	-198.89
103	Bm_{46}	1675.16	38	48.1	7	48.0	612.65	-14.28	1.97	-199.76
104	TG_{10}	1694.96	38	47.2	7	41.4	609.72	-8.44	0.90	-188.77
105	8/1.0	1646.33	38	42.3	7	51.4	622.81	-14.35	0.04	-198.53
106	8/2.0	1640.27	38	42.7	7	51.0	622.76	-16.13	0.12	-199.56
107	8/3.0	1638.20	38	43.2	7	50.7	622.35	-17.05	0.23	-183.08
108	8/4.0	1686.08	38	43.7	7	50.3	611.69	-12.80	0.43	-188.24
109	8/5.0	1687.81	38	44.1	7	50.0	614.27	-9.56	0.44	-188.43
110	8/6.0	1768.12	38	44.5	7	49.7	597.33	-1.59	0.97	-196.88
111	8/6.8	1799.88	38	44.9	7	49.5	589.22	0.20	1.90	-199.51
112	8/8.0	1988.52	38	45.4	7	49.1	550.86	20.22	1.43	-221.14
113	8/9.0	1951.82	38	45.8	7	48.8	557.72	15.88	0.97	-217.44
114	8/10.0	1991.33	38	46.2	7	48.4	551.49	21.96	1.02	-221.81
115	8/11.0	1904.86	38	46.7	7	48.1	566.49	10.41	1.31	-211.85
116	8/12.0	1891.50	38	47.1	7	47.8	563.93	3.85	0.95	-210.71
117	8/13.0	1895.62	38	47.5	7	47.5	568.21	9.54	1.41	-210.71

No	Station	Alt	Longitude	Latitude	G.obs	F.A.	Sg_T	B.A
		m	(deg.min)	(deg.min)	(mgal)	(mgal)	(mgal)	(mgal)
118	8/14.0	1971.36	38 48.0	7 47.1	552.57	17.46	1.13	-219.47
119	8/15.0	2035.84	38 48.4	7 46.8	541.43	26.30	1.13	-226.68
120	8/16.0	2073.91	38 48.8	7 46.5	529.93	26.65	1.45	-230.62
121	8/17.0	2129.82	38 46.2	7 46.2	509.92	24.07	3.34	-234.99
122	8/18.5	1894.88	38 49.9	7 45.7	558.83	0.62	1.14	-210.86
123	Bm_{58}	1638.17	38 43.6	7 51.3	622.16	-17.49	0.2	-183.11
124	Bm_{67}	1653.92	38 44.5	7 51.5	618.62	-16.24	0.31	-184.76
125	Bm_{67A}	1700.58	38 45.9	7 51.6	606.36	-14.16	0.58	-189.71
126	Bm_{68}	1666.98	38 46.8	7 51.8	606.14	-24.83	0.31	-186.23
127	Bm_{69}	1641.75	38 47.8	7 51.3	607.62	-30.93	0.29	-183.42
128	Bm_{70}	1641.39	38 48.7	7 51.0	607.19	-31.37	0.15	-183.52
129	Bm_{71}	1682.16	38 48.3	7 50.0	599.84	-25.73	0.55	-187.68
130	Bm_{72}	1749.50	38 48.2	7 49.0	590.51	-13.88	0.96	-194.81
131	Bm_{73}	1835.75	38 48.1	7 48.6	577.88	0.28	2.09	-203.33
132	Bm_{74}	1927.23	38 47.7	7 48.2	559.69	10.47	0.89	-214.77
133	E_5	1639.40	38 49.8	7 50.8	619.96	-22.39	0.51	-182.94
134	Bm_{83}	1641.05	38 51.0	7 50.4	616.16	-22.23	0.32	-205.54
135	Bm_{84}	1703.63	38 52.1	7 50.6	600.93	-18.26	0.38	-208.51
136	Bm_{85}	1809.29	38 54.0	7 51.3	571.94	-14.92	0.52	-216.86

No.	Station	Alt (m)	Longitude (deg. min)	Latitude (deg. min)	G.obs (mgal)	F.A (mgal)	Sg_T (mgal)	B.A (mgal)
137	Bm_{86}	1765.54	38 55.4	7 52.8	579.64	-21.32	0.25	-218.63
138	Bm_{87}	1714.52	38 56.8	7 54.8	587.37	-30.13	0.21	-221.77
139	Bm_{88}	1787.89	38 57.8	7 53.9	571.18	-23.32	0.31	-223.07
140	Bm_{89}	1900.15	38 58.3	7 52.6	544.38	-14.95	0.43	-223.27
141	Bm_{90}	2014.58	38 59.5	7 51.4	519.65	- 3.89	0.53	-228.79
142	Bm_{90A}	2098.49	38 60.6	7 51.5	500.01	2.35	0.43	-232.04
143	Bm_{91}	2158.75	38 60.9	7 51.3	485.76	6.76	0.36	-234.44
144	Bm_{92}	2173.66	38 60.9	7 50.6	482.02	7.88	0.39	-234.96
145	E_{12}	1602.0	38 48.4	7 43.5	606.06	-41.64	0.09	-220.81
146	E_{13}	1603.0	38 47.9	7 43.5	605.81	-41.58	0.08	-220.88
147	E_{14}	1598.0	38 37.4	7 43.5	604.65	-44.29	0.07	-223.03
148	E_{15}	1594.0	38 36.9	7 43.5	602.41	-47.75	0.05	-226.07
149	E_{16}	1596.0	38 36.4	7 43.6	602.06	-47.53	0.06	-226.06
150	E_{17}	1600.0	38 35.9	7 43.8	598.77	-49.64	0.09	-228.59
151	E_{18}	1596.0	38 35.4	7 43.9	598.64	-51.05	0.1	-229.55
152	E_{19}	1597.0	38 34.9	7 44.0	600.09	-49.35	0.11	-227.93
153	E_{20}	1600.0	38 34.3	7 44.1	599.86	-48.68	0.1	-227.62
154	E_{21}	1599.0	38 33.8	7 44.1	599.32	-49.56	0.09	-228.39
155	E_{22}	1601.00	38 33.33	7 44.1	601.21	-47.05	0.09	-226.11

No	Station	Altitude (m)	Longitude (deg .min)		Latitude (deg. min)		G.obs (mgal)	F.A (mgal)	S_{G_T} (mgal)	B.A (mgal)
156	E_{23}	1600.00	38	32.9	7	44	599.63	-48.90	0.05	-227.89
157	E_{24}	1598.00	38	32.4	7	43.8	597.47	-51.59	0.06	-230.34
158	E_{25}	1602.00	38	32	7	43.6	595.75	-51.97	0.07	-231.17
159	E_{26}	1610.00	38	31.4	7	43.5	597.21	-48.01	0.04	-228.12
160	E_{27}	1617.00	38	30.9	7	43.4	598.90	-44.12	0.08	-224.99
161	E_{28}	1618.00	38	30.4	7	43.3	600.56	-42.13	0.09	-223.09
162	180 E_{29}	1634.6	38	29	7	42.9	599.11	-38.30	0.19	-221.2
163	181	1647.00	38	28.3	7	42.6	598.61	-34.84	0.25	-194.14
164	182	1652.8	38	27.4	7	43.2	597.94	-33.94	0.28	-218.61
165	183	1685	38	26.6	7	43.9	581.37	-30.87	0.32	-219.11
166	E_{31}	1652.00	38	41.8	7	51.6	622.07	-13.44	0.04	-198.25
167	E_{32}	1670.00	38	40.8	7	52.0	625.36	-4 .77	0.05	-191.59
168	E_{33}	1672.00	38	39.7	7	52.0	623.72	-5 .77	0.06	-192.81
169	E_{34}	1683.00	38	38.6	7	52.1	617.14	-8.99	0.08	-197.23
170	E_{35}	1690.00	38	37.6	7	52.3	612.42	-11.63	0.1	-200.64
171	E_{36}	1702.00	38	36.5	7	51.9	610.07	-12.28	0.11	-200.45
172	E_{37}	1710.00	38	35.4	7	51.8	596.06	-23.78	0.09	-212.86
173	E_{38}	1720.00	38	34.6	7	52.3	592.19	-22.62	0.11	-214.97
174	E_{39}	1735.0	38	37.5	7	53.2	583.16	-27.39	0.13	-221.4

No	Station	Alt (m)	Longitude (deg. min)		Latitude (deg. min)		G.obs (mgal)	F.A (mgal)	Sgt (mgal)	B.A (mgal)
175	E_{40}	1662.00	38	39.9	7	49.7	624.80	- 6.86	0.04	-192.79
176	E_{41}	1670.0	38	38.9	7	50	623.18	- 6.15	0.05	-192.97
177	E_{42}	1680.0	38	37.9	7	50.5	619.15	- 7.29	0.04	-195.24
178	E_{43}	1690.0	38	36.9	7	50.9	613.11	-10.40	0.05	-199.45
179	E_{44}	1700.0	38	35.9	7	51.3	604.91	-15.67	0.08	-205.82
180	E_{45}	1736.00	38	33.7	7	52.1	578.52	-31.24	0.10	-225.4
181	E_{46}	1770.00	38	32.9	7	52.3	562.83	-36.53	0.16	-234.43
182	E_{47}	1590.0	38	40.4	7	38.1	606.53	-42.71	0.21	-220.41
183	E_{48}	1601.0	38	39.8	7	37.0	603.07	-42.34	0.21	-221.28
184	E_{49}	1621.0	38	40.2	7	35.9	599.69	-39.11	0.18	-220.31
185	E_{50}	1636.0	38	40.2	7	34.8	595.09	-38.64	0.12	-221.59
186	E_{51}	1638.0	38	40.1	7	33.7	592.49	-40.18	0.13	-223.35
187	E_{52}	1650.0	38	40.0	7	32.4	587.97	-40.46	0.16	-224.88
188	E_{53}	1635.0	38	40.0	7	31.7	588.39	-44.39	0.18	-227.17
189	E_{54}	1625.0	38	40.5	7	31.4	588.67	-47.07	0.19	-228.71
190	E_{72}	1610.5	38	40.8	7	31.3	593.68	-46.5	0.15	-226.56
191	E_{73}	1604.5	38	41.3	7	31.2	597.28	-44.71	0.19	-224.6
192	E_{74}	1600	38	41.8	7	31.2	596.00	-47.39	0.24	-226.19
193	E_{75}	1586	38	42.1	7	40.3	614.82	-36.51	0.25	-213.73

No	Station	Alt (m)	Longitude (deg. min)		Latitude (deg. min)		G.obs. (mgal)	F.A (mgal)	Sg_T (Mgal)	B.A (mgal)
194	E_{76}	1586	38	42.4	7	39.8	614.69	-36.48	0.25	-213.70
195	E_{77}	1586	38	42.3	7	39.5	613.39	-37.63	0.21	-214.89
196	E_{78}	1585	38	42.3	7	39.0	612.19	-39.01	0.12	-216.25
197	E_{79}	1583.5	38	43.6	7	41.6	621.46	-31.18	0.12	-208.26
198	E80	1583.34	38	44	7	41.8	626.63	-26.13	0.21	-203.10
199	E_{81}	1585	38	44.7	7	41.9	631.19	-21.09	0.19	-198.26
200	E_{82}	1585	38	45.2	7	41.3	636.71	-15.35	0.31	-192.40
201	E_{83}	1585	38	45.3	7	40.9	634.63	-17.28	0.35	-194.29
202	E_{64}	1645.00	38	42.6	7	53.2	621.05	-17.25	0.12	-201.2
203	E65	1645.00	38	42.7	7	54.2	616.90	-21.82	0.11	-205.79
204	E_{66}	1646.00	38	42.8	7	55.5	617.63	-21.27	0.13	-205.33
205	E67	1642.00	38	43.0	7	56.9	620.71	-20.02	0.12	-203.63
206	E68	1638.0	38	43.1	7	58.0	615.82	-26.27	0.10	-209.76
207	E_{69}	1642.0	38	43.2	7	59.1	613.39	-28.20	0.09	-211.85
208	E_{70}	1650	38	42.8	7	60.1	609.42	-30.09	0.08	-214.65
209	E_{71}	1660	38	43.2	7	61.0	606.38	-30.43	0.10	-216.08
210	$P_{30}/1.5$	1918.5	38	46.5	7	48.00	559.46	13.09	0.85	-213.83
211	$P_{30}/2.0$	1902.14	38	46.6	7	47.7	564.74	8.00	0.66	-212.19
212	$P_{30}/3.0$	1945.34	38	46.7	7	47.2	562.61	19.40	1.42	-216.26

No	Station	Alt. (m)	Longitude (deg. min)		Latitude (deg.min)		G.obs. (mgal)	F.A (mgal)	Sg_T (mgal)	B.A (mgal)
213	$P_{30}/4.10$	2188.86	38	47.0	7	46.7	502.53	36.65	4.82	-240.11
214	fumerols	2259.20	38	47.1	7	46.5	491.25	45.19	7.55	-245.25
215	$P_{30}/5.0$	2267.93	38	47.1	7	46.2	485.47	42.18	4.51	-249.27
216	P_{30}	2341.19	38	47.2	7	46.0	468.06	47.18	7.00	-254.98
217	$P_{30}/5.9$	2287.04	38	47.3	7	45.8	489.32	52.08	6.74	-249.8
218	$P_{30}/6.7$	2064.26	38	47.4	7	45.3	528.75	22.64	3.59	-227.4
219	$P_{30}/7.70$	1835.75	38	47.6	7	44.9	578.31	1.93	2.61	-202.81
220	$P_{30}/8.16$	1783.54	38	47.7	7	44.6	589.14	- 3.32	2.61	-196.97
221	$P_{30}/00$	1935.77	38	46.1	7	48.8	559.8	13.0	0.95	-215.66
222	$P_{30}/-1.0$	1994.08	38	46.1	7	49.3	548.26	19.25	2.14	-220.86
223	$P_{30}/-1.5$	1938.21	38	46.0	7	49.5	560.49	14.14	1.80	-200.94
224	$P_{30}/-2.0$	1901.39	38	46.0	7	49.8	567.84	10.03	1.50	211.27
225	TG-2	1595.94	38	47.2	7	42.8	632.35	-16.95	1.65	-193.65
226	TG-4	1627.35	38	43.9	7	44.5	617.37	-22.89	2.34	-201.74
227	TG-5	1625.37	38	44.1	7	44.4	616.88	-23.94	2.33	-203.47
228	TG-6	1719.06	38	44.4	7	45.2	599.55	-12.69	1.92	-203.18
229	TG-8	1702.73	38	43.3	7	46.9	605.46	-12.49	1.48	-201.52
230	TG-18	1973.20	38	44.8	7	48.7	552.66	17.42	1.43	-201.95
231	TG-17	1953.00	38	45.6	7	48.1	557.21	16.01	1.43	-201.11

No	Station	Alt (m)	Longitude (deg. min)		Latitude (deg. min)		G.obs (mgal)	F.A (mgal)	Sg_T (mgal)	B.A (mgal)
232	TG-12	1903.45	38	46.6	7	47.9	566.86	10.43	0.7	-201.9
233	TG-16	1894.53	38	47.5	7	47.5	567.40	8.39	1.41	-202.19
234	TG-20	1953.00	38	48.2	7	47.4	557.20	16.28	1.13	-201.13
235	TG-13	1911.48	38	46.7	7	47.4	563.28	9.52	1.10	-203.49
236	TG-22	1931.8	38	47.7	7	48.3	559.07	11.25	0.89	-204.03
237	TG-14A	1854.12	38	48.1	7	48.6	574.44	2.51	2.08	-202.92
238	TG-15	1788.73	38	48.2	7	48.8	584.73	-7.47	1.52	-206.08
239	TG-21	1690.63	38	47.9	7	49.9	598.16	-24.74	0.75	-213.15
240	TG-11	1929.95	38	46.4	7	48.2	562.95	14.59	1.16	-200.24
241	TG-23	1968.00	38	46.02	7	47.42	554.31	-67.6	1.50	-200.73
242	TG-19	1916.11	38	45.78	7	49.13	565.08	12.07	1.78	-200.52
243	E_{84}	1737	38	40.5	7	27.9	572.12	-27.65	0.16	-201.86
244	E_{85}	1677.5	38	40.1	7	29.0	586.32	-32.29	0.15	-219.85
245	E86	1672.00	38	39.6	7	28.8	588.08	-32.13	0.14	-219.09
246	E_{87}	1559	38	38.1	7	28.3	620.78	-34.10	0.25	-208.30
247	E_{88}	1599.00	38	38.5	7	28.5	606.04	-36.58	0.20	-215.31
248	E_{89}	1640	38	39.00	7	28.8	596.17	-33.93	0.21	-217.23
249	E_{90}	1768.5	38	40.4	7	26.6	566.300	-23.25	0.08	-221.07
250	E_{91}	1840	38	40.5	7	25.6	550.05	-17.01	0.09	-222.82

No	Station	Alt (m)	Longitude (deg.min)	Latitude (deg. min)	G.obs (mgal)	F.A (mgal)	Sg_T (mgal)	B.A (mgal)
251	E_{92}	1880.5	38 40.3	7 24.4	540.48	-13.63	0.09	-223.97
252	E_{93}	1900	38 40.3	7 23.3	533.95	-13.71	0.10	-226.22
253	E_{94}	1904.5	38 40.2	7 22.1	531.9	-13.89	0.10	-226.91
254	E_{95}	1925	38 40.1	7 21.2	529.34	- 9.75	0.15	-225.0
255	E_{96}	1937	38 39.8	7 20.1	528.33	- 6.63	0.10	-223.28
256	E_{97}	1921.5	38 39.2	7 19.2	533.21	- 6.15	0.12	-221.05
257	E_{98}	1890	38 38.8	7 17.9	543.69	- 4.88	0.10	-216.27
258	E_{99}	1938	38 39.1	7 16.8	535.08	.1.74	0.11	-215.01
259	E_{100}	1976.5	38 39.1	7 15.2	529.55	8.73	0.10	-212.34
260	E_{101}	1961	38 38.3	7 14.3	519.21	- 6.01	0.09	-225.36
261	E_{102}	1967	38 37.6	7 13.5	525.25	2.21	0.08	-217.82
262	E_{103}	1942	38 37.1	7 12.8	533.58	3.09	0.08	-214.14
263	E_{104}	1928.5	38 35.7	7 11.7	537.1	2.90	0.07	-212.83
264	E_{105}	1585	38 41.9	7 36.2	603.81	-46.19	0.10	-223.45
265	E_{106}	1980.00	38 41.1	7 20.6	519.61	- 2.28	0.19	-223.65
266	E_{107}	2020.00	38 42.1	7 20.1	517.92	8.60	0.23	-217.21
267	E_{108}	2036.5	38 43.1	7 19.6	517.15	13.10	0.21	-214.57
268	E_{109}	2095.6	38 44.1	7 19.1	503.07	17.47	0.40	-216.63
269	E_{110}	2108	38 45.2	7 18.9	498.75	17.05	0.51	-218.32
270	E_{111}	2104.5	38 46.2	7 18.8	500.77	18.03	0.62	-216.84
271	E_{112}	2120	38 47.1	7 18.7	494.03	16.10	0.70	-220.42
272	E_{113}	2160	38 48.1	7 18.1	486.21	20.87	0.91	-219.92
273	E_{114}	2180	38 48.6	7 18.3	478.75	19.51	0.95	-223.48
274	E_{115}	2130	38 48.1	7 19.6	491.93	16.76	0.92	-220 .67

No	Station	(m)	Longitude (deg. min)		Latitude (deg. min)		G.obs (mgal)	F.A (mgal	Sgt (mgal)	B.A (mgal)
275	E_{116}	2110	38	48.7	7	20.3	495.75	14.09	0.90	-221.12
276	E117	2128.5	38	49.6	7	20.9	495.68	19.51	1.02	-217.65
277	E_{118}	2113.5	38	50.2	7	21.6	499.73	18.64	1.20	-216.66
278	E_{119}	2106	38	50.6	7	22.6	502.78	19.00	0.81	-215.85
279	E_{120}	2107	38	50.8	7	23.4	497.11	13.30	0.71	-221.76
280	E_{121}	2090	38	50.4	7	24.3	506.51	17.08	0.62	-216.17
281	E_{122}	2064	38	50.1	7	25.1	509.65	11.87	0.81	-218.28
282	E_{123}	1888	38	19.7	7	46.4	564.77	35.02	0.21	-206.89
283	E_{124}	1931	38	18.9	7	47.0	554.32	6.78	0.23	-209.07
284	E125	1950	38	17.8	7	47.6	547.61	5.67	0.22	-212.32
285	E_{126}	1968	38	16.7	7	47.6	541.57	5.19	0.20	-214.83
286	E127	1940	38	15.7	7	47.6	541.17	-3.87	0.25	-220.70
287	E_{128}	1943	38	14.7	7	47.4	536.82	-7.21	0.26	-224.37
288	E_{129}	1875	38	34.9	7	12.7	552.41	1.27	0.08	-208.46
289	E_{130}	1847	38	34.0	7	13.2	558.96	-1.01	0.10	-207.59
290	E_{131}	1812	38	32.8	7	13.5	567.58	-3.32	0.14	-205.94
291	E_{132}	1785	38	31.7	7	14.2	576.47	-3.04	0.20	-202.58
292	E_{133}	1771	38	30.6	7	14.6	585.09	1.09	0.15	-196.93
293	E_{134}	1697.5	38	29.4	7	15.3	601.02	-5.92	0.21	-195.66
294	E_{135}	1696.5	38	28.0	7	16.1	605.67	-1.90	0.22	-191.51
295	E_{136}	1691	38	27.2	7	16.5	607.02	-2.42	0.15	-191.50
296	E137	1698	38	26.2	7	17.1	603.39	-4.11	0.12	-194.00
297	E_{138}	1856	38	20.3	7	17.9	551.10	-7.96	0.14	-215.40
298	E_{139}	1846.7	38	21.2	7	17.8	562.41	0.53	0.10	-206.01

No	Station	Alt (m)	Longitude (deg. min)		Latitude (deg. min)		G.obs (mgal)	F.A (mgal)	Sg_T (mgal)	B.A (mgal)
299	E_{140}	1786.7	38	22.5	7	17.7	577.05	- 3.30	0.08	-203.16
300	E_{141}	1790.0	38	20.1	7	38.5	572.92	-14.75	0.16	-216.41
301	E_{142}	1784.0	38	20.4	7	37.2	572.16	-16.85	0.13	-216.25
302	E_{143}	1799.0	38	20.4	7	36.1	569.83	-14.12	0.10	-215.33
303	E_{144}	1806	38	20.0	7	34.9	565.28	-15.98	0.13	-217.94
304	E_{145}	1677.8	38	24.5	7	17.2	611.80	- 1.99	0.19	-189.55
305	E146	1911.00	38	19.1	7	17.5	539.01	- 2.94	0.25	-216.53
306	E147	1903.50	38	17.7	7	17.2	542.68	- 1.46	0.28	-214.18
307	E_{148}	1902.60	38	16.3	7	17.0	545.69	1.35	0.31	-221.24
308	E_{149}	1894.00	38	15.1	7	16.9	547.57	0.63	0.28	-211.03
309	E_{150}	1873.50	38	13.8	7	17.0	549.64	- 3.67	0.26	-213.05
310	E_{151}	1878.00	38	12.6	7	17.2	553.23	1.23	0.19	-208.72
311	E_{152}	1772.50	38	5.5	7	18.6	580.48	- 4.65	0.10	-202.89
312	E_{153}	1780.00	38	6.2	7	21.5	575.80	- 8.17	0.04	-207.31
313	E_{154}	1782.00	38	5.7	7	20.5	576.47	- 6.49	0.08	-205.81
314	E_{154}	1782.00	38	5.3	7	19.5	579.11	- 3.43	0.05	-202.79
315	E_{156}	1782.50	38	6.9	7	18.6	575.63	- 6.39	0.10	-205.75
316	E_{157}	1792.50	38	7.9	7	18.4	574.61	- 4.25	0.08	-204.75
317	E_{158}	1818.00	38	9.1	7	18.1	568.03	- 2.85	0.09	-206.19
318	E_{159}	1845.5	38	10.2	7	17.8	563.22	1.57	0.10	-205.06
319	E_{160}	1866.50	38	11.6	7	17.4	557.57	1.93	0.08	-206.85
320	E_{161}	1862.50	38	10.5	7	18.8	558.86	1.43	0.02	-206.96
321	E_{162}	1881.50	38	10.6	7	19.9	557.14	5.13	0.08	-205.33
322	E_{163}	1900.50	38	10.2	7	20.9	556.43	9.88	0.09	-202.70

No	Station	Alt (m)	Longitude (deg. min)	Latitude (deg.min)	G.obs (mgal)	F.A (mgal)	Sg_T (mgal)	B.A (mgal)
323	E_{164}	1925.50	38 10.2	7 21.8	553.51	14.32	0.10	-201.05
324	E_{165}	1958.00	38 10.8	7 22.5	551.05	21.61	0.18	-197.31
325	E_{166}	2040.00	38 11.3	7 23.7	531.46	26.85	0.26	-201.16
326	E_{167}	1595.00	38 36.0	7 43.3	600.53	-49.23	0.08	-227.[illegible]
327	E_{168}	1590.00	38 34.9	7 43.0	600.42	-50.76	0.07	-228.61
328	E_{169}	1589.00	38 33.8	7 42.5	601.80	-49.52	0.05	-227.[illegible]
329	E_{170}	1586.00	38 33.0	7 42.4	602.51	-49.69	0.06	-227.10
330	E_{171}	1594.00	38 32.0	7 42.0	602.04	-47.52	0.09	-225.80
331	E_{172}	1596.00	38 31.1	7 41.4	606.75	-41.96	0.10	-220.[illegible]
332	E_{173}	1598.00	38 30.2	7 40.8	612.74	-35.10	0.11	-213.[illegible]
333	E_{174}	1604.0	38 28.9	7 40,3	621.38	-24.43	0.12	-203.[illegible]
334	E_{175}	1603.0	38 27.8	7 40.1	624.09	-21.95	0.13	-201.[illegible]
335	E_{176}	1603.0	38 26.7	7 40.0	621.97	-24.00	0.10	-203.[illegible]
336	E_{177}	1623.0	38 25.7	7 39.9	614.57	-25.20	0.08	-206.[illegible]
337	E_{178}	1660	38 24.5	7 39.9	596.65	-31.69	0.09	-217.[illegible]
338	E_{179}	1746	38 23.5	7 40.1	577.34	-24.56	0.10	-219.[illegible]
339	E_{180}	1773	38 22.5	7 40.5	571.59	-22.12	0.11	-220.[illegible]
340	E_{181}	1799	38 20.6	7 40.9	572.15	-13.70	0.12	-214.[illegible]
341	E_{182}	1805	38 19.5	7 40.9	571.45	-12.55	0.10	-214.[illegible]
342	E_{183}	2015.5	38 37.3	7 11.5	514.75	8.16	0.05	-218.0[illegible]
343	E_{184}	2070.6	38 38.6	7 11.2	502.31	12.86	0.02	-219.[illegible]
344	E_{185}	2167.5	38 39.6	7 10.7	479.95	20.60	0.04	-222.60
345	E_{186}	2291.7	38 40.6	7 9.7	452.46	31.85	0.06	-225.2[illegible]
346	E_{187}	2346.5	38 41.7	7 9.1	431.63	31.16	0.04	-232.07

No	Station	Alt (m)	Longitude (deg.min)		Latitude (deg. min)		G.obs (mgal)	F.A (mgal)	Sg_T (mgal)	B.A (mgal)
347	E_{189}	2443.5	38	42.6	7	8.2	413.07	39.90	0.06	-234.17
348	E_{190}	2503.5	38	43.5	7	7.2	394.65	40.40	0.12	-240.32
349	E_{191}	2554.5	38	44.5	7	6.2	378.03	39.89	0.12	-246.54
350	E_{192}	2627.5	38	45.6	7	5.3	362.08	46.84	0.12	-247.75
351	E_{193}	2676.5	38	47.0	7	4.6	353.59	53.74	0.23	-246.23
352	E_{194}	2069.5	38	12.3	7	24.2	521.99	26.27	0.09	-205.22
353	E_{195}	2045.5	38	13.1	7	25.1	522.05	18.58	0.10	-210.22
354	E_{196}	2060.0	38	13.5	7	26.1	518.30	18.89	0.16	-211.46
355	E_{197}	2007.0	38	14.0	7	27.1	528.91	12.75	0.15	-211.68
356	E_{198}	1964.5	38	14.5	7	28.0	535.73	6.10	0.21	-213.52
357	E_{199}	1914.5	38	14.4	7	29.1	545.69	0.21	0.18	-213.85
358	E_{200}	1832.5	38	15.0	7	29.8	561.26	-9.8	0.19	-214.67
359	E_{201}	1669	38	28.8	7	16.4	607.97	-8.19	0.12	-194.83
360	E_{202}	1666	38	28.1	7	17.2	609.87	-7.55	0.13	-193.84
361	E_{203}	1673	38	27.4	7	18.0	603.34	-12.25	0.08	-199.38
362	E_{204}	1671	38	26.4	7	18.7	604.72	-11.74	0.09	-198.64
363	E_{205}	1695	38	25.6	7	19.4	598.88	-10.47	0.07	-200.07
364	E_{206}	1672	38	25.5	7	20.5	604.33	-12.55	0.06	-199.59
365	E_{207}	1671.5	38	25.5	7	21.7	603.74	-13.72	.10	-200.66
366	E_{208}	1671.5	38	25.6	7	22.6	604.12	-13.78	.06	-200.76
367	E_{209}	1600	38	25.7	7	23.7	614.82	-25.57	.02	-204.59
368	E_{210}	1567.5	38	25.7	7	24.8	614.64	-36.22	.07	-211.55
369	E_{211}	1560	38	25.3	7	25.2	626.71	-26.63	0.12	-201.08
370	A	1756	38	56.2	7	55.6	577.70	-27.32	0.12	-223.70

No	Station	Alt (m)	Longitude (deg. min)	Latitude (deg.min)	G.obs (mgal)	F.A (mgal)	Sg_T (mgal)	B.A (mgal)
371	A_2	1672	38 55.5	7 57.5	596.99	-34.69	0.10	-221.69
372	A_3	1720	38 54.4	7 57.2	592.70	-24.06	0.08	-216.45
373	A_4	1637	38 53.7	7 57.6	615.71	-26.81	0.15	-209.78
374	A_5	1637	38 53.4	7 57.9	618.73	-23.93	0.09	-207.08
375	A_8	1675	38 48.4	7 43.5	607.92	-17.26	0.82	-199.44
376	A_7	1697	38 49.1	7 43.5	601.26	-17.11	0.95	-203.74
377	A_8	1704	38 51.8	7 49.3	599.67	-18.88	0.45	-206.55
378	A_9	1761	38 52.7	7 49.0	582.07	-18.74	0.63	-215.19
379	A_{11}	1861	38 58.1	7 52.4	551.96	-19.36	0.10	-227.50
380	A12	1874	38 56.6	7 51.3	546.83	-20.03	0.15	-229.58
381	A_{13}	1884	38 56.1	7 50.5	546.22	-17.24	0.16	-227.9
382	A_{14}	1871	38 55.3	7 49.9	548.31	-18.91	0.15	-228.13
383	A_{15}	1882	38 54.2	7 48.0	546.2	-16.90	0.12	-227.38
384	A_{16}	1899	38 53.0	7 46.2	544.03	-13.11	0.16	-225.45
385	A_{27}	1585	38 26.5	7 37.6	627.88	-22.67	0.21	-199.83
386	A28	1743.0	38 22.0	7 19.5	581.17	-13.41	0.08	-208.37
387	A_{29}	1668.0	38 22.9	7 22.8	596.47	-21.77	0.05	-208.37
388	A_{30}	1636.0	38 23.6	7 22.3	604.0	-24.72	0.04	-207.74
389	A_{31}	1577.0	38 24.1	7 23.8	619.96	-27.57	0.07	-203.97
390	A_{32}	1558.0	38 24.5	7 24.9	628.77	-25.05	0.06	-199.33
391	A_{33}	1796.0	38 20.7	7 19.0	565.21	-12.82	0.04	-213.75
392	A_{34}	1786.0	38 20.5	7 20.6	572.17	- 9.57	0.05	-209.38
393	A_{35}	1810.0	38 20.5	7 21.6	567.4	- 7.35	0.09	-209.80
394	A_{36}	1802.0	38 19.1	7 22.6	562.65	-14.56	0.08	-216.12

No	Station	Alt (m)	Longitude (deg. min)	Latitude (deg.min)	G.obs (mgal)	F.A (mgal)	S_{g_T} (mgal)	B.A (mgal)
395	A_{37}	1807.0	38 17 7	22.6	561.31	-14.78	0.05	-216.93
396	A_{38}	1800	38 16.8 7	23.7	563.13	-15.55	0.15	-216.82
397	A_{212}	1865.5	38 23.2 7	44.5	558.76	- 8.01	0.35	-216.41
398	A_{39}	1831	38 15.2 7	21.3	559.84	- 8.29	0.18	-213.00
399	E_{213}	1838	38 22.6 7	42.7	561.94	-12.62	0.30	-217.99
400	E_{214}	1815	38 22.3 7	42.0	564.03	-17.35	0.40	-220.05
401	E_{215}	1809	38 21.9 7	41.3	566.96	-15.98	0.31	-218.9
402	E_{216}	1821.5	38 21.5 7	41.3	566.1	-12.98	0.22	-216.58

D E C L A R A T I O N

I, the undersigned declare that the thesis is my original work and has not been presented for a degree in any other University. All sources of materials used for the thesis have been duly acknowledged.

Name ABERA ALEMU

Signature 

Place and date of submission:

The thesis is submitted to the Physics Department Graduate Comittee, on June 9, 1983.